



Bachelor Thesis

Ethylenediamine based PA Thin-Film Composite Membrane for Separation of Salty Water

Study programme:

B3942 Nanotechnology

Study branch:

Nanomaterials

Author:

Vojtěch John

Supervisor:

doc. Fatma Yalcinkaya, Ph.D., M.Sc.

Institute of Mechatronics and Computer Engineering

Liberec 2022



Bachelor Thesis Assignment Form

Ethylenediamine based PA Thin-Film Composite Membrane for Separation of Salty Water

<i>Name and surname:</i>	Vojtěch John
<i>Identification number:</i>	M18000128
<i>Study programme:</i>	B3942 Nanotechnology
<i>Study branch (specialization):</i>	Nanomaterials
<i>Assigning department:</i>	Institute of Mechatronics and Computer Engineering
<i>Academic year:</i>	2022/2023

Rules of Elaboration:

1. Fabricate a thin-film nanofibrous composite membrane using ethylenediamine (EDA) and trimethyl chloride (TMC).
2. Measure the effect of low pH on the separation process.
3. Measure the effectivity of the separation of monovalent and divalent salts.
4. Characterise the prepared membranes

Scope of Graphic Work: by appropriate documentation
Scope of Report: 30–40 pages
Thesis Form: printed/electronic
Thesis Language: English

List of Specialised Literature:

- [1] Yalcinkaya, B., Yalcinkaya, F. and Chaloupek, J., 2017. Optimisation of thin film composite nanofiltration membranes based on laminated nanofibrous and nonwoven supporting material. *Desalination and Water Treatment*, 59, pp.19-30.
- [2] Shaari, N.Z.K., Sulaiman, N.A. and Abd Rahman, N., 2019. Thin film composite membranes: Preparation, characterization, and application towards copper ion removal. *Journal of Environmental Chemical Engineering*, 7(1), p.102845.
- [3] Lau, W.J., Ismail, A.F., Misdan, N. and Kassim, M.A., 2012. A recent progress in thin film composite membrane: A review. *Desalination*, 287, pp.190-199.
- [4] Lihong, W.A.N.G., Deling, L.I., Cheng, L., Zhang, L. and Huanlin, C.H.E.N., 2011. Preparation of thin film composite nanofiltration membrane by interfacial polymerization with 3, 5-diaminobenzoylpiperazine and trimesoyl chloride. *Chinese Journal of Chemical Engineering*, 19(2), pp.262-266.
- [5] Yalcinkaya, B., Yalcinkaya, F. and Chaloupek, J., 2016. Thin film nanofibrous composite membrane for dead-end seawater desalination. *Journal of Nanomaterials*, 2016.

Thesis Supervisor: doc. Fatma Yalcinkaya, Ph.D., M.Sc.
Institute of Mechatronics and Computer
Engineering

Date of Thesis Assignment: October 12, 2022
Date of Thesis Submission: May 15, 2023

prof. Ing. Zdeněk Plíva, Ph.D.
Dean

doc. Ing. Josef Černohorský, Ph.D.
Head of institute

Declaration

I hereby certify, I, myself, have written my bachelor thesis as an original and primary work using the literature listed below and consulting it with my thesis supervisor and my thesis counsellor.

I acknowledge that my bachelor thesis is fully governed by Act No. 121/2000 Coll., the Copyright Act, in particular Article 60 – School Work.

I acknowledge that the Technical University of Liberec does not infringe my copyrights by using my bachelor thesis for internal purposes of the Technical University of Liberec. I am aware of my obligation to inform the Technical University of Liberec on having used or granted license to use the results of my bachelor thesis; in such a case the Technical University of Liberec may require reimbursement of the costs incurred for creating the result up to their actual amount.

At the same time, I honestly declare that the text of the printed version of my bachelor thesis is identical with the text of the electronic version uploaded into the IS STAG. I acknowledge that the Technical University of Liberec will make my bachelor thesis public in accordance with paragraph 47b of Act No. 111/1998 Coll., on Higher Education Institutions and on Amendment to Other Acts (the Higher Education Act), as amended. I am aware of the consequences which may under the Higher Education Act result from a breach of this declaration.

August 20, 2023

Vojtěch John

Acknowledgements

I would like to thank my supervisor, doc. Fatma Yalcinkaya, Ph.D., M.Sc., for her support, help and guidance through my study, research, and experiments conducted and, most importantly, the motivation needed to finish this thesis.

I would also like to express my gratitude and love to my family and my closest friends, without whom I would never be the person I am.

A big thanks to the Material Research Team for being great friends.

A special thank you to Ing. Michaela Petržílková and Ing. Jana Müllerová, Ph.D. for their goodwill in helping with different analyses.

Last but not least, I would like to acknowledge the assistance provided by the Research Infrastructure NanoEnviCz (Project No. LM2023066), supported by the Ministry of Education, Youth and Sports of the Czech Republic.

Abstract

This thesis focuses on the preparation of a polyamide (PA) thin film composite membrane by applying ethylenediamine (EDA) and trimesoyl chloride (TMC) monomers onto a nanofibrous layer. The primary objective of this thesis is to develop composite thin-film membranes for the efficient separation of saline water. To achieve this objective, the following steps are taken: (a) the concentration of EDA monomer required for optimisation, (b) the optimisation of the monomers immersion time and the optimisation of the interval between the immersions. Blending with a further water-soluble monomer (PIP), (c) enhancing the hydrophilic characteristics of the surface of a nanofiber support layer, (d) the optimisation of time for curing.

In this experiment, sodium chloride (NaCl) and magnesium sulphate (MgSO_4) are both subjected to a rejection test. Initial membrane preparation results revealed lower-than-anticipated rejection rates for both NaCl and MgSO_4 , necessitating a systematic optimisation approach. In particular, alterations in monomer concentration, reaction durations, and monomer combinations provided insight into modifiable membrane performance parameters. The study demonstrated that rejection rates as high as 84.95 % for MgSO_4 and 83.53 % for NaCl are achievable through iterative refinements. In addition, the study investigated the effect of pH, revealing a significant increase in rejection capabilities at lower pH values.

The optimal membranes were selected based on their capacity to reject salt efficiently. Due to the increased complexity associated with the separation of monovalent NaCl salt, the elimination of NaCl salt is our primary focus. The selected membranes were subsequently subjected to further characterisation. This research advances membrane technology for efficient water purification, especially in desalination processes.

Keywords: thin-film composite membranes, desalination, filtration, interfacial polymerisation

Abstrakt

Tato práce se zaměřuje na přípravu kompozitní tenkovrstvé membrány z polyamidu (PA) aplikací monomerů ethylendiaminu (EDA) a trimesoylchloridu (TMC) na vrstvu z nanovláken. Hlavním cílem této práce je vyvinout kompozitní tenkovrstvé membrány pro efektivní separaci soli z vody. K dosažení tohoto cíle jsou podniknuty následující kroky: (a) stanovení optimální koncentrace monomeru EDA, (b) optimalizace doby reakce monomerů a optimalizace intervalu mezi dvěma monomery. Smísení s dalším vodou rozpustným monomerem (PIP), (c) zlepšení hydrofilních vlastností povrchu nanovlákněné podpůrné vrstvy, (d) optimalizace doby pro vytvrzení.

V tomto experimentu jsou chlorid sodný (NaCl) a síran hořečnatý ($MgSO_4$) podrobeny testu selektivity. Počáteční výsledky přípravy membrán ukázaly nižší než očekávané míry selektivity jak pro NaCl, tak pro $MgSO_4$, což vyžadovalo systematický přístup k optimalizaci. Zvlášť změny koncentrace monomeru, doby reakce a kombinací monomerů poskytly náhled na modifikovatelné parametry efektivity membrány. Studie ukázala, že opakovanými úpravami lze dosáhnout míry odmítnutí až 84,95 % pro $MgSO_4$ a 83,53 % pro NaCl. Kromě toho studie zkoumala účinek pH a odhalila významný nárůst schopnosti odmítnutí při nižších hodnotách pH.

Optimální membrány byly vybrány na základě schopnosti účinně odfiltrovat sůl. Kvůli zvýšené složitosti spojené s odstraňováním jednovaletní soli NaCl je našim hlavním zájmem eliminace soli NaCl. Vybrané membrány byly následně podrobeny další charakterizaci. Tato studie posunuje technologii membrán pro efektivní čištění vody, zejména v procesech odsolování.

Klíčová slova: tenkovrstvé kompozitní membrány, odsolování, filtrace, mezifázová polymerizace

Contents

Declaration	2
Acknowledgements.....	5
Abstract	6
Abstrakt.....	7
Contents	8
List of figures	10
List of tables	11
List of abbreviations	12
1. Introduction.....	13
2. Theoretical part.....	14
2.1 Membranes.....	14
2.2 Pressure-driven membrane separation processes	14
2.3 Types of membranes	15
2.3.1 Asymmetric membranes	15
2.3.2 Electrically charged membranes	15
2.3.3 Thin-film composite (TFC)	15
2.4 Membrane materials for desalination.....	15
2.4.1 Organic materials	16
2.4.2 Inorganic materials	16
2.5 Thin-film composite membranes.....	17
2.6 Ethylenediamine as a functional component.....	18
2.6.1 EDA - Graphene oxide membrane	18
2.6.2 EDA - Metal-organic framework membrane	18
2.6.3 EDA - MXene membrane	19
2.6.4 EDA - PA membranes	19
2.7 Ethylenediamine-based PA membranes	20
2.7.1 Polyamide (PA) polymerization.....	20
2.7.2 EDA-based membranes for water treatment	21
2.8 TFC membrane structure	22

2.9 Gaps in existing literature	23
2.10 Aim of the thesis	24
3. Experimental part	25
3.1 Materials and methods	25
3.1.1 Materials	25
3.1.2 Methods	25
3.2 Membrane synthesis	26
3.3 Changes in the original procedure	27
3.3.1 Changes in the contact times	27
3.3.2 Modifications of the monomers	28
3.3.3 Modifications of the support material	28
3.3.4 Further optimisation	29
4. Results and Discussion	30
4.1 Results of filtration tests	30
4.2 Results of pH change	36
4.3 The Analysis of Film Morphology and Composition using Scanning Electron Microscopy (SEM)	38
4.4 Surface Chemical Property	40
4.5 Contact angle	41
4.6 Further research	44
5. Conclusion	44
References	46

List of figures

Figure 2.1: Pressure-driven separation processes	11
Figure 2.2: Polyamide polymerization derived from (a) EDA and TMC, (b) PIP and TMC.	16
Figure 2.3: Composition of a TFC membrane	19
Figure 2.4: Schematic diagram for dead-end ultrafiltration membrane process.....	22
Figure 4.1: Comparison of flux and rejection rates for different feeds	26
Figure 4.2: Comparison of flux and rejection rates for different contact and drying times	27
Figure 4.3: Comparison of flux and rejection rates for different modifications	28
Figure 4.4: Comparison of flux and rejection rates between modified and unmodified support	29
Figure 4.5: Comparison of flux and rejection rates for different surfactants	30
Figure 4.6: Comparison of flux and rejection rates for monomer solution used multiple times in a row	31
Figure 4.7: Comparison of flux and rejection rates for samples made with a focus on identical conditions.....	32
Figure 4.8: Comparison of flux and rejection rates of the best-performing samples with commercially available membranes	33
Figure 4.9: FTIR images EDA/TMC formed PA thin-film	37

List of tables

Table 4.1: Comparison of flux and rejection rates for different feeds	26
Table 4.2: Comparison of flux and rejection rates for different contact and drying times	27
Table 4.3: Comparison of flux and rejection rates for different modifications	28
Table 4.4: Comparison of flux and rejection rates between modified and unmodified support	29
Table 4.5: Comparison of flux and rejection rates for different surfactants	30
Table 4.6: Comparison of flux and rejection rates for monomer solution used multiple times in a row	31
Table 4.7: Comparison of flux and rejection rates for samples made with a focus on identical conditions.....	32
Table 4.8: Comparison of flux and rejection rates of the best-performing samples with commercially available membranes	34
Table 4.9: List of samples chosen for further analysis	35
Table 4.10: SEM images of samples A, D and E	36
Table 4.11: Images of contact angles of chosen samples	39
Table 4.12: List of contact angle values of chosen samples	39

List of abbreviations

BPA	Bisphenol A
EDA	Ethylenediamine
Et	Ethanol
FO	Forward osmosis
FTIR	Fourier transform infrared spectroscopy
GO	Graphite oxide
CHD	1,4-cyclohexane
IC	Isophthaloyl chloride
IP	Interfacial polymerisation
LMH	Litres per squared meter per hour
MOF	Metal-organic framework
MPDA	m-phenylene diamine
MST	Membrane separation technology
NF	Nanofiltration
PA	Polyamide
PIP	Piperazine
PVA	Polyvinyl alcohol
RO	Reverse osmosis
SDS	Sodium dodecyl sulphate
SEM	Scanning electron microscopy
TC	Terephthaloyl chloride
TMC	1,3,5-trimesoyl chloride
UAE	United Arab Emirates
WCA	Water contact angle

1. Introduction

Water is an essential component of all life on Earth. It functions as a medium for almost every chemical reaction within our bodies. It serves as a solvent which enables our bodies to transport all nutrients, hormones, enzymes and gases throughout our bodies. Water is needed for photosynthesis to take place in green plants and algae. Photosynthesis then produces oxygen for all of us to breathe.

Although two-thirds of the earth's surface is covered in water, only a fraction is drinkable. The scarcity of drinkable water is a culprit in economics, geopolitics and one of the reasons for people's migration. Water cycles continuously in the hydrosphere in a somewhat predictable manner. However, climate changes, whether caused by human influence or not, render all predictions less accurate. Some places are struck by droughts, massive forest fires, dust storms and suffer from desertification. Some places receive far more rainfall causing flooding and soil degradation. Both cases, hand to hand with pollution caused by human activity, call for a sustainable and reliable way of purifying our drinking and utility water [1–4].

A great source of water is the ocean. Many countries are currently using big desalination plants. There are about 21 000 of them all around the world with the biggest being in Saudi Arabia, UAE and Israel. These plants can purify large amounts of water supplying over 300 million people. However, even though energy efficiency has improved ten times since 1970, desalination plants still represented 25 % of the energy consumed by the water sector in 2016.

Finding a more sustainable means of desalination and water treatment should be a priority. With new materials and methods for the fabrication of membranes, new highly selective membranes can be used as an alternative that doesn't require as much energy and is much cheaper to use. Regarding installed capacity growth, the current leading process is reverse osmosis which uses semipermeable membranes combined with applied pressure [5–7]. For these reasons, this thesis aims at broadening our understanding of a new viable monomer usable in the process of desalination via membrane filtration and modifications for enhancing the efficiency of said membranes.

2. Theoretical part

2.1 Membranes

Membranes can be defined as barriers that separate two phases - the feed and the permeate. These phases are part of a process in which materials from the feed solution are selectively transferred through the membrane, creating the permeate solution. This transfer occurs due to various driving forces such as pressure, concentration differences, or temperature gradients. To function effectively, a membrane must possess a mechanism that allows the transport of one component of the feed while blocking the transport of the other [8, 9].

In the context of porous membranes, this mechanism often revolves around the size of the pores, allowing only particles of specific sizes to pass through. Conversely, non-porous membranes rely on the chemical affinities between the feed components and the membrane material.

2.2 Pressure-driven membrane separation processes

A membrane filtration process can be described as the separation of a feed stream by a membrane into a concentrate fraction and a permeate fraction. The pressure gradient is used as the driving force for pushing the solvent through the membrane. Particles and dissolved components are kept partially based on their size, shape, and charge.

Microfiltration, ultrafiltration, nanofiltration, and reverse osmosis are the four types of pressure-driven membrane processes that may be categorised according to the pore size of the membrane in decreasing order [10]. The ranges of particle sizes for different processes are shown in Figure 2.1.

Apart from the processes mentioned above, there are many more membrane separation processes which utilise membrane separation in combination with a different separation process such as membrane distillation [8].

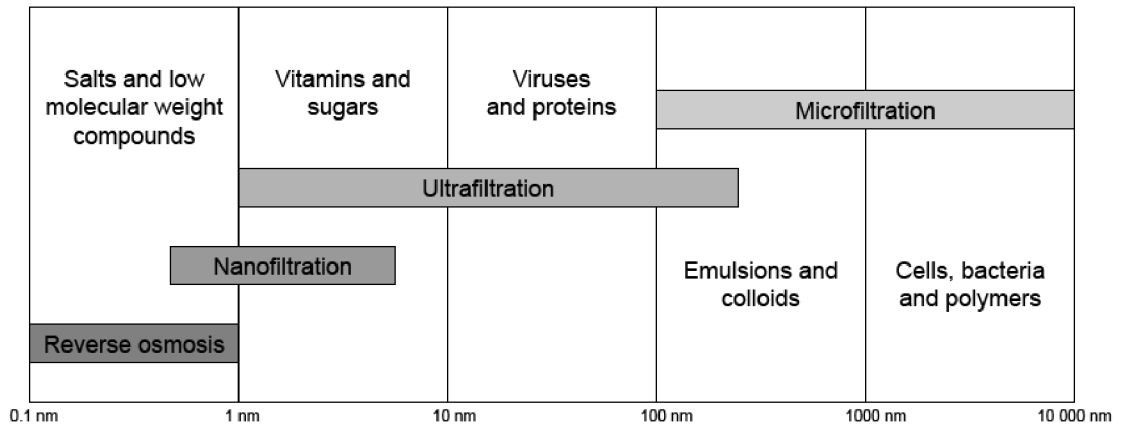


Figure 2.1: Pressure-driven separation processes [8]

2.3 Types of membranes

2.3.1 Asymmetric membranes

This type of membrane is characterised by thin skin on the surface of the membrane. The layers underneath the skin provide structural support. The pore size determines separation characteristics and the rate of mass transport is dependent on the thickness of the skin.

2.3.2 Electrically charged membranes

Ion exchange membranes are mostly microporous materials. They consist of swollen gels. Pore walls have a fixed charge that binds ions from the surrounding fluid feed. Depending on which charge is carried within the membrane, the membranes are referred to as either anion exchange or cation exchange membranes.

2.3.3 Thin-film composite (TFC)

TFC membranes are primarily used in reverse osmosis and nanofiltration for water treatment. These composites are made of a thin and dense polymer layer formed on a microporous support material. TFC membrane fabrication and its properties will be more closely discussed in the chapter **Thin-film composite membranes**. [8]

2.4 Membrane materials for desalination

Compared to conventional methods of separation of salt from salinated water like distillation, membrane separation technology (MST) offers notable advantages. MST has

gained substantial attention in recent years due to its potential to meet energy demands and promote sustainable green development. Its primary benefits over traditional separation methods include high separation accuracy, low energy requirements, cost effectiveness, and a reduced carbon footprint. In the desalination industry, thin film composite (TFC) membranes, particularly those utilising reverse osmosis, are prevalent. These membranes typically consist of a dense polyamide layer created through an interfacial polymerisation (IP) reaction and a porous support layer. [11, 12]

Ideally, a perfect membrane would allow the desired substance to flow through at the highest rate while completely blocking unwanted substances. However, there's often a trade-off between permeability and selectivity in most membrane materials. Generally, higher permeability corresponds to lower selectivity and rejection rates. To address this issue, nanomaterials and various surface modifications are being incorporated.

2.4.1 Organic materials

The IP reaction offers a significant advantage by allowing separate preparation of the support layer and the active layer, facilitating easier optimization of membrane selectivity. Common monomers used in the aqueous phase include piperazine (PIP), polyvinyl alcohol (PVA), and bisphenol A (BPA). In the organic phase, frequently used monomers comprise isophthaloyl chloride (IC), terephthaloyl chloride (TC), and 1,3,5-trimesoyl chloride (TMC). [11]

2.4.2 Inorganic materials

In addition to organic materials, several inorganic materials are employed for membrane production. Inorganic membranes are categorised based on the materials used, such as metal membranes, ceramic membranes, and glass membranes. In desalination and gas separation, notable attention is given to materials like MXene, graphene oxides, and Molybdenum disulfide (MoS_2) membranes.

MXene materials consist of transition metals, nitrides, carbides, or carbonitrides. These are synthesised through a top-down selective hydrofluoric acid etching process, resulting in a multi-layer or few-layer MXene structure with an accordion-like morphology. MXene membranes find applications in desalination and gas separation due to their

adjustable layer spacing and hydrophilicity, achieving high water permeability and salt rejection [11, 13, 14].

Graphite oxide (GO) is a stable, highly hydrophilic material obtained by oxidising graphene at a low cost. Nanoporous graphene oxide sheets are stacked, with pore diameter determined by interlayer distance. Channels formed by these stacked layers allow water to permeate while rejecting other substances [15, 16].

MoS₂ is another prominent material for membrane fabrication. MoS₂ nanosheets have even stronger molecular interactions than graphene oxides. Stacked MoS₂ nanosheets enable water permeation while excluding chloride and sodium ions. Similar to GO, this material forms channels for rapid water passage while blocking other substances [17, 18].

2.5 Thin-film composite membranes

Thin-film composite (TFC) membranes find extensive applications, including reverse osmosis (RO), forward osmosis (FO), and nanofiltration (NF). They are known for their ease of fabrication, exceptional selectivity, and acceptable permeability. A TFC membrane consists of a thin selective film integrated with a porous and mechanically robust support material. This unique structure allows for separate optimization of both components. The fabrication process involves saturating the support material with an aqueous solution containing monomer A. Subsequently, the support is brought into contact with an organic solution containing monomer B. Typically, monomer A has much higher solubility in the organic solvent than monomer B has in the aqueous solution. The interfacial polymerization is rapidly decelerated as the polymer film forms. This occurs due to the film's role in preventing contact between phases, leading to a self-terminating reaction [19, 20].

While TFC membranes tend to exhibit remarkable selectivity, they often display lower water permeability. Studies diverge on whether a support material with smaller or larger pores is more suitable for achieving higher TFC membrane permeability. Additional factors that could influence permeability include material hydrophobicity and the composition of support material fibres, such as whether they are hollow or solid. Many researchers associate water permeability with the thickness of the polyamide film.

Thinner films allow for less polyamide penetration into the support material, resulting in higher permeability [21–23].

Scanning electron microscopy (SEM) is commonly employed to examine PA TFC membranes. Nevertheless, the surface of the film is uneven, making accurate determination of the film's thickness challenging. This rugged surface comprises globular features, and high-resolution SEM has confirmed that these features consist of fully-aromatic polyamide films. These globular formations are filled with water when fully hydrated [24].

2.6 Ethylenediamine as a functional component

2.6.1 EDA - Graphene oxide membrane

Ethylenediamine (EDA) stands out due to its possession of primary amine groups on both ends of its chain structure. This heightened reactivity differentiates it from counterparts like piperazine (PIP), which features two secondary amine groups. This superior reactivity is believed to contribute to a higher cross-linking density, thereby enhancing separation performance. EDA has been effectively employed in functionalising a graphene oxide (GO) hollow fibre membrane. The resulting GO-EDA membrane exhibited exceptional performance, marked by high CO₂ permeance and remarkable CO₂/N₂ selectivity. This positions it as a strong contender for CO₂ separation applications [25].

2.6.2 EDA - Metal-organic framework membrane

Moreover, EDA forms coordination complexes with heavy metal ions, rendering it a promising contender for heavy metal removal from wastewater. Metal-organic framework (MOF) membranes functionalized with EDA have demonstrated up to 95% efficiency in removing Pb, up to 90% efficiency for Cd, and 80% efficiency for Cu. Adjusting the pH of the feed solution further improves removal efficiency, with higher pH levels enhancing the affinity of metal ions to EDA. However, it's worth noting that while higher pH increases separation efficiency, MOF structures tend to collapse in basic conditions. Notably, GO-EDA exhibits commendable regeneration potential and stability,

maintaining consistent removal efficiency even after four adsorption-desorption cycles [26].

2.6.3 EDA - MXene membrane

The functionalisation of MXene $Ti_3C_2T_x$ with EDA has also been explored for heavy metal removal from wastewater. Remarkably high rejection rates were achieved, reaching up to 99.8% for metals such as Mn, Zn, Cd, Cu, Ni, and Pb. Interestingly, optimal efficiency was attained at lower pH feed solutions, with the highest effectiveness recorded at pH 3. Notably, increasing pH had a negligible negative impact. Changes in the concentration of heavy metal ions in the feed displayed minimal influence on the overall rejection rate. Additionally, the nanofiltration performance exhibited stability even when processing substantial feed volumes; the initial rejection rate remained consistent even after 5000 ml of operation. Coupled with its easy fabrication, the performance of MXene-EDA makes it an appealing candidate for wastewater treatment purposes [27].

2.6.4 EDA - PA membranes

EDA serves as a valuable modifier for polyamide thin-film composite (TFC) membranes as well. In the development of reverse osmosis (RO) membranes, a significant challenge lies in enhancing anti-fouling capabilities. Fouling can arise either from chemical sources, primarily due to the deposition of inorganic materials, or from biological factors, involving the attachment and growth of various microbes and bacteria. To address this issue, an EDA aqueous solution has been applied to a membrane based on m-phenylene diamine (MPDA) PA.

In its pristine state, an MPDA PA membrane exhibits a contact angle of approximately 60° . Upon modification with EDA, this angle reduces to around 45° . While this change has led to a slight decrease in salt rejection, it has concurrently resulted in a substantial (30%) increase in water permeability. Notably, during fouling experiments, the EDA-modified membrane displayed the capability to maintain 99% permeability, in comparison to the unmodified membrane which, within the same duration, experienced a reduction to 78% permeability [28].

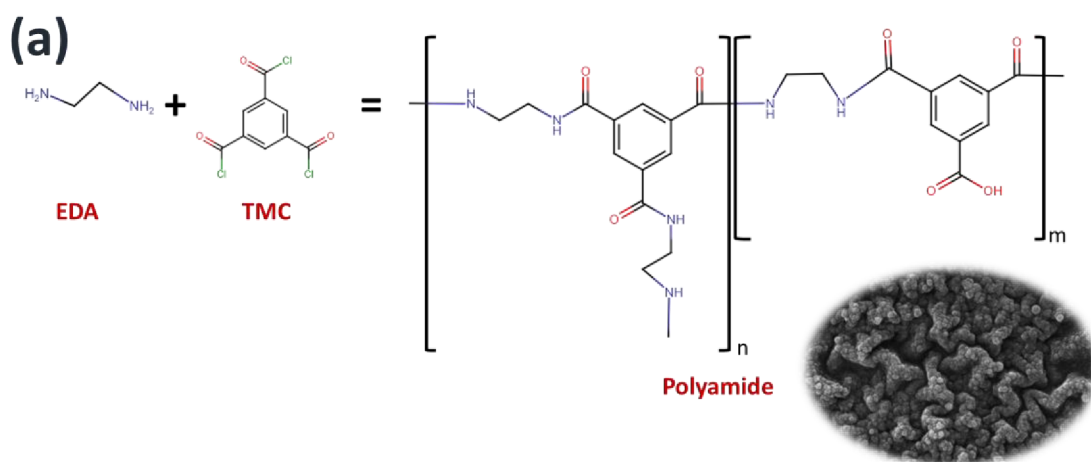
2.7 Ethylenediamine-based PA membranes

2.7.1 Polyamide (PA) polymerization

The diamines exhibited variations in their chemical composition, with the distinguishing factor being the type of functional group located between the terminal amines. The aliphatic group found in ethylenediamine (EDA) and the aromatic or benzene ring present in m-phenylene diamine (MPDA) were the two classifications seen. EDA possesses a brief linear alkane chain, allowing it to easily react with TMC and afterwards create a remarkably dense and selective layer. The chemical structure of EDA consists of alkane moieties with terminal groups composed of diamine.

Nanofiltration (NF) membranes consist of a partially crosslinked, semi-aromatic PA material that is formed through the interfacial polymerization of TMC and PIP. The PIP-based thin-film composite membrane is classified as an "open" or "loose" NF membrane.

The characteristics of the polyamide layer, including its surface shape, roughness, and thickness, are influenced by the reaction of the diamines. Figure 2.2 illustrates the proposed mechanism for polyamide synthesis, which involves the combination of EDA-TMC monomers and PIP-TMC monomers. The reaction illustrates the interaction between acyl chloride groups present in TMC and NH_2 groups found in EDA on the surface. This contact leads to the creation of amide bonds and the release of HCl molecules as byproducts during the polycondensation reaction [29, 30]



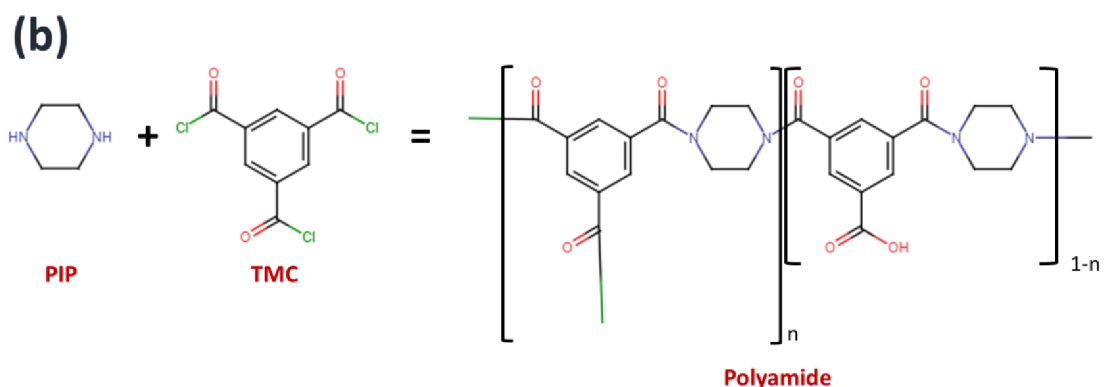


Figure 2.2: Polyamide polymerization derived from (a) EDA and TMC, (b) PIP and TMC.

2.7.2 EDA-based membranes for water treatment

To explore the broader utility of EDA in desalination and water treatment, a comparative analysis was carried out involving various amine-based monomers. Monomers featuring diverse functional groups, including triethylenetetramine (TETA), piperazine (PIP), meta-phenylenediamine (MPD), and EDA, were subjected to an interfacial polymerization (IP) reaction with TMC. The membranes produced through this process were subsequently evaluated for both permeation properties and simultaneously their ability to remove arsenic from water and desalinate seawater.

The EDA-TMC membrane exhibited a permeability of approximately 5 LMH (litres per square metre per hour). Notably, the PIP-TMC membrane outperformed the EDA-TMC membrane with a permeability of 7 LMH. The other membranes demonstrated comparable permeabilities but with somewhat more significant deviations. The removal of both arsenic and NaCl from water showed consistent results across all tested membranes, reaching a peak of 99.9%. [31]

In an additional study, it was observed that the interfacial polymerization of EDA with TMC results in the formation of a relatively thicker polyamide layer, measuring approximately 95.3 ± 3.27 nm. Interestingly, this thickness is three times greater than that of a membrane based on 1,4-cyclohexane diamine (CHD), which was employed for comparative purposes.

The study also revealed that when subjected to a pH of 3, the EDA-based membrane exhibited a higher positive charge compared to its CHD-based counterpart, implying a greater presence of cross-linked amide groups. Despite these characteristics, the EDA-based membrane's salt rejection rate was approximately 50%, notably lower than the up to 90% observed for the CHD-based membrane. Moreover, the EDA-based membrane displayed a permeability for pure water that was two times lower than its CHD-based counterpart. [32]

2.8 TFC membrane structure

Thin film composite (TFC) membranes have witnessed rapid advancements since the introduction of interfacial polymerisation (IP) techniques. These membranes hold great potential for diverse separation applications, particularly within wastewater treatment processes. A TFC membrane consists of two essential components: an active polyamide (PA) film and a highly porous support material. The majority of research emphasises the active PA film formed during the IP reaction. Various monomers with distinct chemical properties, including cross-linking capabilities, functional groups, and bonds, are employed. The overall performance of the membrane is intricately tied to the final structure of the film, encompassing factors such as pore size, thickness, roughness, and hydrophilicity. [33]

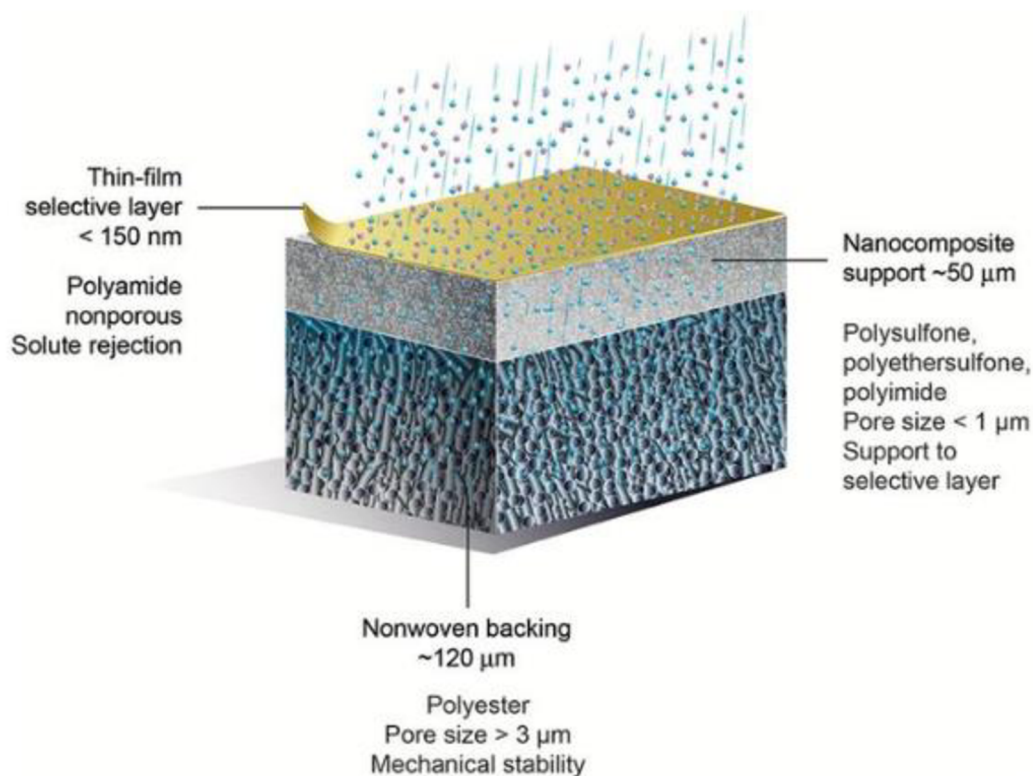


Figure 2.3: Composition of a TFC membrane [34]

In addition to the choice of monomers, the morphology of the support material and its compatibility with various amidic monomers are crucial factors. Furthermore, different materials may be better suited for specific applications. One approach to modify the behaviour of the support material involves introducing a surfactant into the aqueous solution during the IP reaction. The integration of a suitable surfactant can facilitate the movement of the monomer into the support material, thus enhancing the overall membrane properties. This surfactant-based modification improves the adhesion between the components. It holds the potential to prevent undesired swelling, which could occur under certain conditions and decrease the functionality of the membrane. [33, 35]

2.9 Gaps in existing literature

The majority of studies focused on thin film composite (TFC) membranes tend to explore various monomers such as meta-phenylenediamine (MPD) or piperazine (PIP). These monomers have demonstrated remarkable efficacy in wastewater treatment and water desalination applications [31]. Ethylenediamine (EDA), on the other hand, has exhibited its potential as a modifier for other polyamide or even inorganic membranes, showcasing

its ability to enhance permeability and anti-fouling properties [28]. However, the broader potential of EDA as a foundational monomer for TFC membranes, especially in combination with 1,3,5-trimesoyl chloride (TMC), remains relatively under-researched.

Another significant area that warrants increased research involves EDA-based TFC membranes that are modified by other monomers or materials. This could include pre-modifying monomers before the interfacial polymerisation (IP) reaction, employing multiple consecutive polymerisation steps to fabricate stacked polyamide layers, or enhancing the EDA membrane through the incorporation of diverse nanoparticles. This approach holds the potential for tailoring membranes with advanced functionalities and improved performance characteristics.

2.10 Aim of the thesis

This thesis focuses on the preparation of a thin film composite membrane composed of polyamide (PA) employing ethylenediamine (EDA) and trimesoyl chloride (TMC) monomers, which are deposited onto a nanofibrous layer. The primary aim of this thesis is to produce thin film composite membranes with the intention of achieving efficient separation of saline water. To attain this purpose, the following actions are implemented:

- The concentration of EDA monomer for optimization purposes.
- The optimisation of the reaction time for monomer immersion.
- The optimization of the period between two monomers in a monomer reaction.
- Blending with an additional aqueous-based monomer (PIP),
- The process of enhancing the hydrophilic properties of the surface of a support nanofiber layer.
- The optimization of curing time

This experiment involves doing a rejection test on two distinct salts, namely sodium chloride (NaCl) and magnesium sulphate (MgSO₄). The objective is to examine the influence of pH on both the rejection and flow rates.

The optimal membranes were chosen based on their ability to effectively reject salt. Due to the increased complexity associated with the separation of monovalent NaCl salt, our primary emphasis is directed at the removal of NaCl salt. The membranes that were chosen were subsequently subjected to additional characterisation.

3. Experimental part

3.1 Materials and methods

3.1.1 Materials

The support material used in this thesis is a nanofibrous membrane with $0.41 \pm 0.02 \mu\text{m}$ sized pores. It comprises 3 g/m² polyamide nanofibers on 80 g/m² polyethylene/polypropylene (20/80) bicomponent nonwoven. PA active layer was made via IP reaction with the use of ethylenediamine (99% pure) from Sigma-Aldrich, 1,3,5-Benzenetricarbonyl trichloride (98% pure) from Aldrich, n-Hexane (95% pure) from Penta chemicals unlimited and distilled water. Dodecyl sulfate sodium salt from Sigma-Aldrich and ethanol absolute (99.8%) were used as surfactants. Piperazine (99%) was used for the modification of selected samples. Salt feeds were prepared with anhydrous magnesium sulfate (98%+) and sodium chloride from Penta chemicals unlimited. The commercially available support material was Whatman® membrane filters nylon, pore size 0.45 μm , diam. 47 mm and the commercially available filter used for comparison was Sterlitech polyamide6 polymeric Flat Sheet Membrane used in reverse osmosis for the separation of salt ions from water.

3.1.2 Methods

3.1.2.1 Filtration test

For each set of membranes tested in the membrane cell of the lab-scale dead-end apparatus (Figure 2), at least two samples were evaluated. The membranes were subjected to pre-compaction at a pressure of 4 bar for a duration of 1 hour using distilled water. Subsequently, the water flux (f) of saline water was quantified at 4 bar by recording the total volume of the water in the permeate (l) throughout a specified duration (t). The salt rejection rate was measured by introducing a solution containing 2000 parts per million (ppm) of salts. The permeate collection was conducted to assess the salt rejection of NaCl and MgSO₄ using a conductometer Orion STAR A112 from Thermo SCIENTIFIC. The calculations for permeability and salt rejection were performed using Equations (1) and (2).

$$f = \frac{l}{At} [\text{Lm}^{-2}\text{h}^{-1}] \quad (1)$$

$$R = \frac{C_f - C_p}{C_f} \times 100\% \quad [\%] \quad (2)$$

where A is the effective membrane area (m^2), R is the rejection of salt (%), C_f is the conductivity of feed, and C_p is the conductivity of permeate.

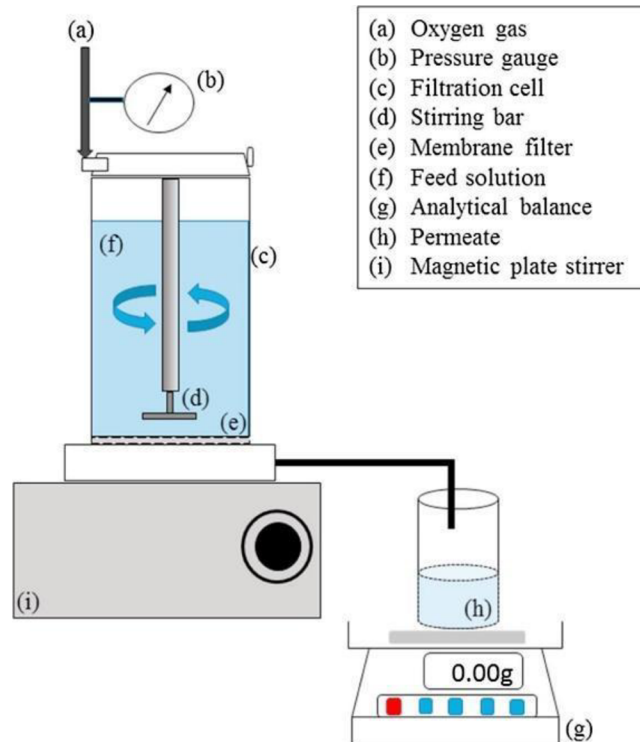


Figure 2.4: Schematic diagram for dead-end ultrafiltration membrane process [36].

3.1.2.2 Membrane Characterization

Fourier-transform infrared spectroscopy (FTIR, Nicolet iZ10 by Thermo Scientific) was used to determine the thin-film layer. The layer is prepared without support. The surface morphology of the prepared samples was investigated by using SEM image (UHR-SEM Zeiss Ultra Plus). The water contact angle of the membranes was determined by employing the Krüss Drop Shape Analyser DS4 (Krüss GmbH, Hamburg, Germany) in conjunction with distilled water, which had a surface tension of 72.0 mN m^{-1} .

3.2 Membrane synthesis

In order to prepare the thin film composite membrane, two solutions were used. Solution A consisted of a 2% solution of ethylenediamine (EDA) dissolved in distilled water. Solution B consisted of a 0.2% solution of trimesoyl chloride (TMC) dissolved in n-hexane. TMC exists in solid form at room temperature, so both the TMC and the n-hexane needed to be preheated to at least 50°C . After preparing both solutions, a magnetic stirrer was added to each respective container, and the solutions were stirred for approximately

30 minutes. After this time, a visual inspection was conducted to check for any impurities and/or undissolved particles in the solutions. If either of the solutions were contaminated, a new solution would be prepared.

After both solutions were thoroughly mixed and visually confirmed to be free of impurities, each solution was transferred to its respective petri dish. A sample of nonwoven PA6 nanofiber textile was first introduced to solution A. Due to the surface tension of the dry textile and its buoyancy, the sample needed to be held submerged in the solution. After 90 seconds, the sample was taken out and left to dry, resting against a wall of a glass container layered with paper, for 180 seconds. After the drying period, the sample was introduced to solution B. Now submerged by its own weight, the sample was left in the solution for another 90 seconds. Then, the sample was taken out, placed between two aluminium rings for support, and put in an oven set to 100 °C for 10 minutes. When completely dry, the sample was transferred to a plastic container filled with distilled water and placed in a refrigerator to protect it from bacteria.

3.3 Changes in the original procedure

3.3.1 Changes in the contact times

To explore the potential of EDA as a suitable monomer for this application, changes were made to the preparation process. The salt rejection testing would now only be conducted with the MgSO₄ solution to test as many samples as possible in a shorter time. The first change was an increase in polymerisation times. The samples would now be submerged in solution A for 300 seconds, followed by a 60-second drying period. Then, the samples were submerged in solution B for 120 seconds and dried in the oven for 10 minutes at 100 °C. This change resulted in an even lower efficiency of 17 %.

Another change was an increase in the length of the resting period between two monomers. The submersion times for both solutions were reverted to the original 90 seconds, and the resting period was now set to 300 seconds.

3.3.2 Modifications of the monomers

For the next set of samples, the timings were returned to the original 90-180-90 sequence for solution A, drying period, and solution B. The first two samples were used as a control group. For two samples solution A was prepared as a 1:1 mixture of EDA and piperazine (PIP) as a 2% solution in water, while the last two samples had solution B prepared as a 0.2% solution of TMC in xylene instead of n-hexane.

The next step involved changing the concentration of the solutions. Solution A was increased to a concentration of 2.5%, while solution B was increased to 0.5%. Additionally, another resting period was introduced at the end of the preparation sequence, and the timings were adjusted once again. Moreover, concerns were raised about the high temperature in the oven potentially degrading the organic membrane, leading to a change in the temperature as well.

The new sequence became 300 - 60 - 180 - 60 for solution A, drying period, solution B, and another drying period before drying in the oven at 60 °C for 20 minutes.

3.3.3 Modifications of the support material

For testing the effectiveness of support material modification two samples were submerged into a container with 150 ml of distilled water and one drop of ethanol. The conditions of fabrication were then the same as with the previous samples (2.5% EDA, 0.5% TMC with 300 - 60 - 180 - 60 sequence). Two samples were fabricated for reference without the support material modification and two samples were prepared with doubled concentration (5% EDA, 1% TMC).

To further improve the support modification, two different solutions were used. One solution consisted of 150 ml of distilled water and 1 ml of ethanol, and the other solution consisted of 150 ml of distilled water and 0.1 g of sodium dodecyl sulphate (SDS). Again, samples were submerged into these solutions for at least 24 h before the IP reaction. The preparation sequence remained the same: 300 - 60 - 180 - 60, with drying in the oven at 60 °C for 20 minutes. A subsequent test was conducted using lower concentrations of the

pretreatment solutions. For the same amount of water, only 0.5 ml of ethanol and 0.05 g of SDS were used.

3.3.4 Further optimisation

During the process of improving the pretreatment method, the concentrations of the preparation solutions were lowered back to 2% EDA for solution A and 0.2% TMC for solution B. The oven drying duration and temperature were adjusted to 15 minutes at 80 °C.

Both solutions A and B were measured to exactly 10 ml so that each sample had approximately the same amount of monomer. Additionally, a new unused solution was used for each sample and solution B was kept at 50 °C throughout the whole process. The goal was to create membranes that were as homogeneous as possible.

To investigate the effect of lower pH on the rejection rate of the membrane, another test was conducted. A small amount of hydrochloric acid was added to both the MgSO₄ solution and the same volume of distilled water, reducing the pH of both solutions to 3. To further investigate the impact of lower pH on the rejection rate, additional samples were prepared and tested. The first two samples were subjected to a solution with a pH level of 1.7. The second batch of samples was tested at a slightly higher pH of 2.9.

4. Results and Discussion

4.1 Results of filtration tests

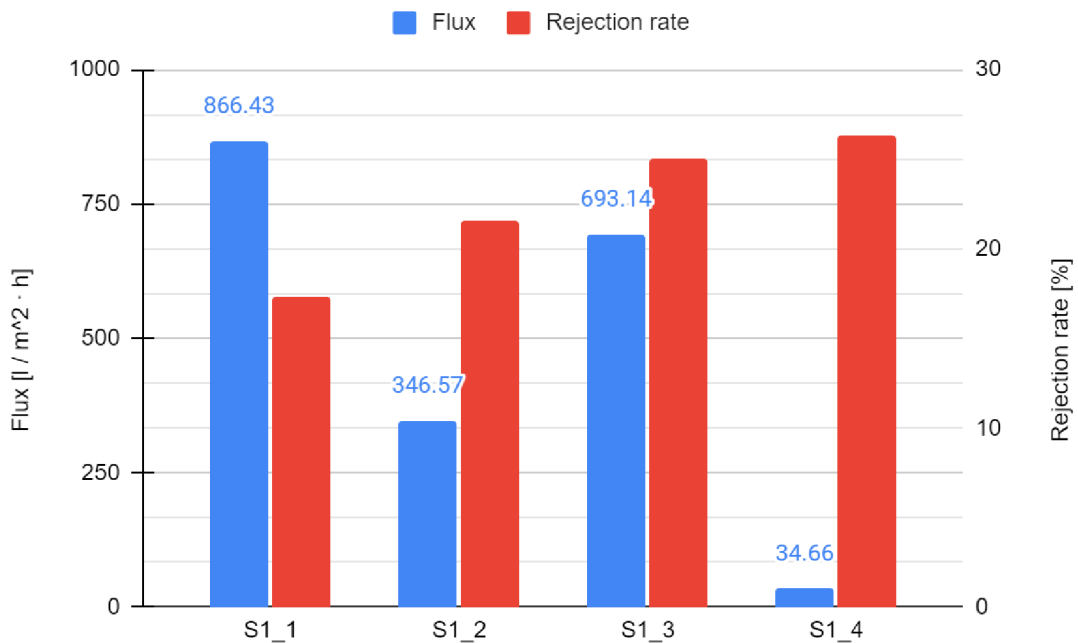


Figure 4.1: Comparison of flux and rejection rates for different feeds

Sample	Solution 1	Solution 2	Contact T S1*	Drying time	Contact T S2*	Drying conditions	Salt feed
S1_1	2 % EDA	0.2 % TMC	90 s	180 s	90 s	10 min @ 100 °C	MgSO ₄
S1_2	2 % EDA	0.2 % TMC	90 s	180 s	90 s	10 min @ 100 °C	MgSO ₄
S1_3	2 % EDA	0.2 % TMC	90 s	180 s	90 s	10 min @ 100 °C	NaCl
S1_4	2 % EDA	0.2 % TMC	90 s	180 s	90 s	10 min @ 100 °C	NaCl

* Contact times with solutions 1 and 2, respectively.

Table 4.1: Comparison of flux and rejection rates for different feeds

The very first samples did not show satisfactory results. While other studies show rejection rates of EDA-based membranes to be around 50 % [32], rejection of only around 20 % was initially achieved with the first samples as seen in Figure 4.1. This fact prompted a series of changes and subsequent tests in order to find better conditions for the fabrication of EDA-based TFC membranes used for water treatment.

Flux rates and rejection rates seemed randomly distributed. They were not apparently affected by the choice of feed, the concentration of the monomers used in the IP reaction or by the contact time of the support material with the monomers as seen in Figure 4.2. Another attempt to increase the efficiency was the modification of said monomers. Two

samples were left with the standard procedure, two samples used a mix of EDA and piperazine (PIP), which was previously tested in the same application and has shown excellent results [9]. The last two samples used xylene as an organic solvent for the organic phase monomer rather than the usual n-hexane.

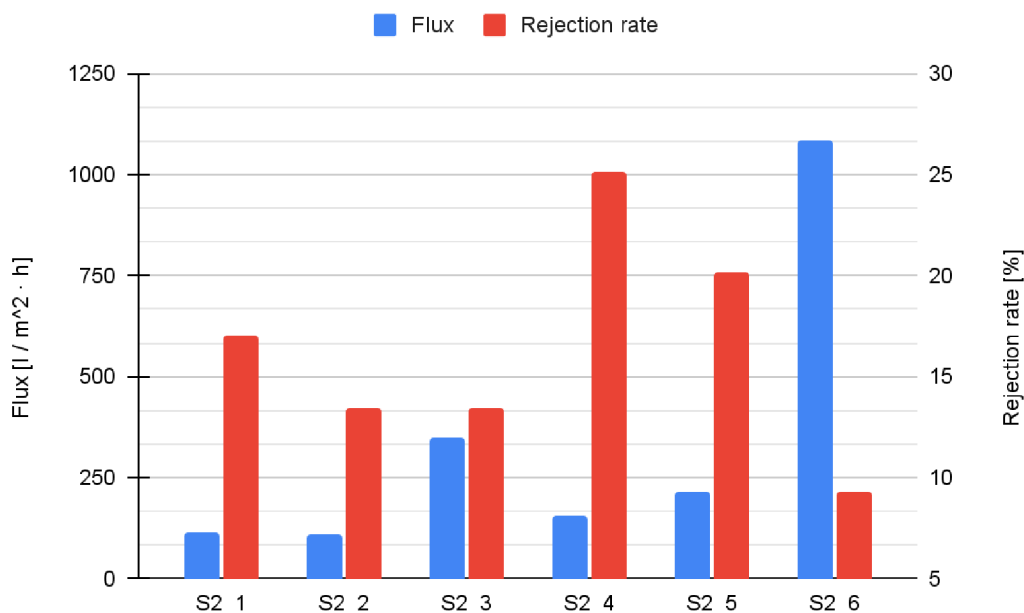


Figure 4.2: Comparison of flux and rejection rates for different contact and drying times

Sample	Solution 1	Solution 2	Contact T S1*	Drying time	Contact T S2*	Drying conditions
S2_1	2 % EDA	0.2 % TMC	300 s	60 s	120 s	10 min @ 100 °C
S2_2	2 % EDA	0.2 % TMC	300 s	60 s	120 s	10 min @ 100 °C
S2_3	2 % EDA	0.2 % TMC	90 s	300 s	90 s	10 min @ 100 °C
S2_4	2 % EDA	0.2 % TMC	90 s	300 s	90 s	10 min @ 100 °C
S2_5	2 % EDA	0.2 % TMC	90 s	180 s	90 s	10 min @ 100 °C
S2_6	2 % EDA	0.2 % TMC	90 s	180 s	90 s	10 min @ 100 °C

* Contact times with solutions 1 and 2, respectively.

Table 4.2: Comparison of flux and rejection rates for different contact and drying times

Both modifications resulted in even lower rejection rates as seen in Figure 4.3. Membranes modified by xylene became sticky and were heavily damaged during removal from the testing apparatus. Even if the resulting rejection rates were better, this would prevent the cleaning and reuse of the membranes. Membranes modified with PIP had very

low rejection rates. Both modifications were deemed undesirable and any further monomer modifications were ruled out.

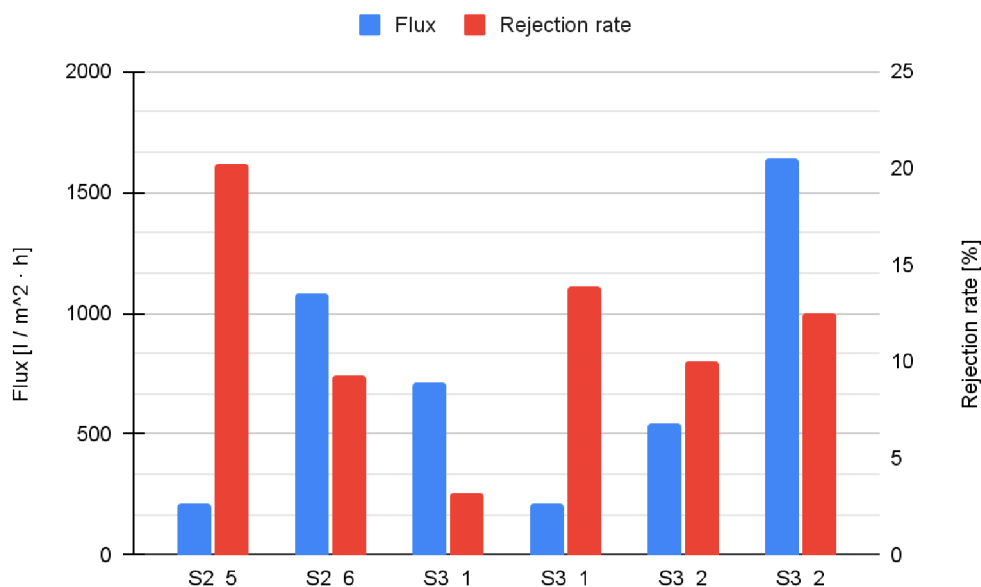


Figure 4.3: Comparison of flux and rejection rates for different modifications

Sample	Solution 1	Solution 2	Contact T S1*	Drying time	Contact T S2*	Drying conditions
S3_1	2 % EDA	0.2 % TMC	90 s	180 s	90 s	10 min @ 100 °C
S3_2	2 % EDA	0.2 % TMC	90 s	180 s	90 s	10 min @ 100 °C
S3_3	2% EDA + PIP	0.2 % TMC	90 s	180 s	90 s	10 min @ 100 °C
S3_4	2% EDA + PIP	0.2 % TMC	90 s	180 s	90 s	10 min @ 100 °C
S3_5	2 % EDA	0.2 % TMC (Xylene)	90 s	180 s	90 s	10 min @ 100 °C
S3_6	2 % EDA	0.2 % TMC (Xylene)	90 s	180 s	90 s	10 min @ 100 °C

* Contact times with solutions 1 and 2, respectively.

Table 4.3: Comparison of flux and rejection rates for different modifications

As seen in Figure 4.4, a sudden change in the rejection rates came with the modification of the support material. Two samples were used for reference, two samples used double concentration of both monomers and for two samples the support material had been submerged in distilled water for 24 hours before the IP reaction itself. While the samples with doubled concentration showed slightly better removal rates, the PA layer itself was very fragile and got torn fairly easily. Samples with modified support material on the other hand showed great rejection when compared to any previous attempts. Tiny air bubbles caught in the support material while it was submerged in the aqueous monomer prompted this alteration of the process. The air bubbles were thought to prevent the monomer from properly coming into contact with the support material and thus creating weak spots in the final membrane. The effects of modifications of the support materials

were discussed by Lau et al., (2012). These modifications could possibly lead to more durable PA films with higher efficiency [33].

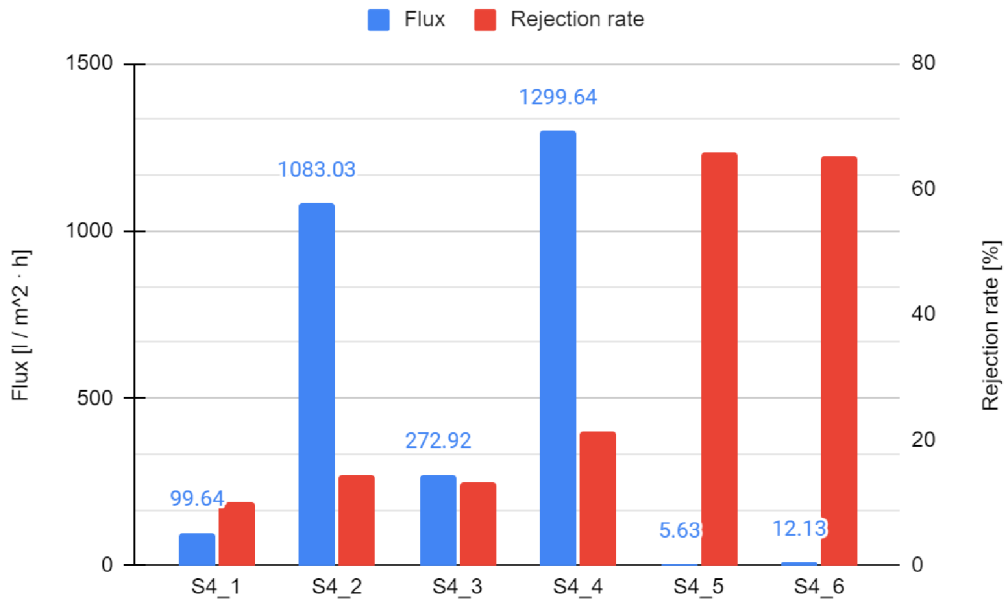


Figure 4.4: Comparison of flux and rejection rates between modified and unmodified support

Sample	Solution 1	Solution 2	Contact T S1*	Drying time	Contact T S2*	Drying conditions	Modification
S4_1	2.5 % EDA	0.5 % TMC	300 s	60 s	180 s	20 min @ 60 °C	None
S4_2	2.5 % EDA	0.5 % TMC	300 s	60 s	180 s	20 min @ 60 °C	None
S4_3	2.5 % EDA	0.5 % TMC	300 s	60 s	180 s	20 min @ 60 °C	None
S4_4	2.5 % EDA	0.5 % TMC	300 s	60 s	180 s	20 min @ 60 °C	None
S4_5	2.5 % EDA	0.5 % TMC	300 s	60 s	180 s	20 min @ 60 °C	Support material soaked in DI water for 24 h
S4_6	2.5 % EDA	0.5 % TMC	300 s	60 s	180 s	20 min @ 60 °C	Support material soaked in DI water for 24 h

* Contact times with solutions 1 and 2, respectively.

Table 4.4: Comparison of flux and rejection rates between modified and unmodified support

Support material modification was deemed as a step in a good direction. To further test its capabilities, two surfactants were tested. Both ethanol and SDS were used in small concentrations with distilled water. As seen in Figure 4.5, SDS did not show any improvement over ethanol while being slightly more challenging to operate with. For this reason, it was not used anymore.

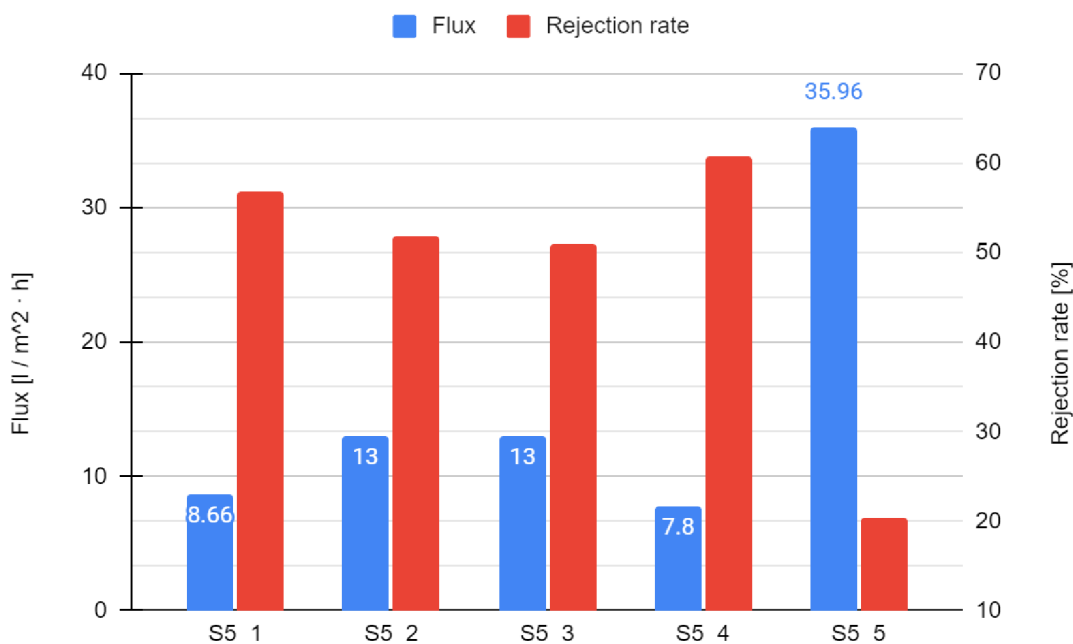


Figure 4.5: Comparison of flux and rejection rates for different surfactants

Sample	Solution 1	Solution 2	Contact T S1*	Drying time	Contact T S2*	2nd drying time	Drying conditions	Surfactant concentration
S5_1	2.5 % EDA	0.5 % TMC	300 s	60 s	180 s	60 s rest	20 min @ 60 °C	0.67 %V Ethanol
S5_2	2.5 % EDA	0.5 % TMC	300 s	60 s	180 s	60 s rest	20 min @ 60 °C	0.07 %w SDS
S5_3	2.5 % EDA	0.5 % TMC	300 s	60 s	180 s	60 s rest	20 min @ 60 °C	0.33 %V Et.
S5_4	2.5 % EDA	0.5 % TMC	300 s	60 s	180 s	60 s rest	20 min @ 60 °C	0.33 %V Et.
S5_5	2.5 % EDA	0.5 % TMC	300 s	60 s	180 s	60 s rest	20 min @ 60 °C	0.035 %w SDS

* Contact times with solutions 1 and 2, respectively.

Table 4.5: Comparison of flux and rejection rates for different surfactants

Samples prepared with the exact same steps and conditions often showed results with great deviations. One monomer solution was up until now used for two samples. As shown in Figure 4.6, samples prepared with the already-used monomer had rejection rates lower by approximately 60 %. However, no samples before the introduction of the support material modification showed signs of this. This could potentially further indicate a better introduction of the monomer to the support thanks to the modification as there is now not enough monomer left in the aqueous solution after the first use. Figure 4.7 shows two membranes prepared with a focus on identical conditions during the fabrication. This was

done to show the option of making EDA-based membranes set to some standard for rejection rate.

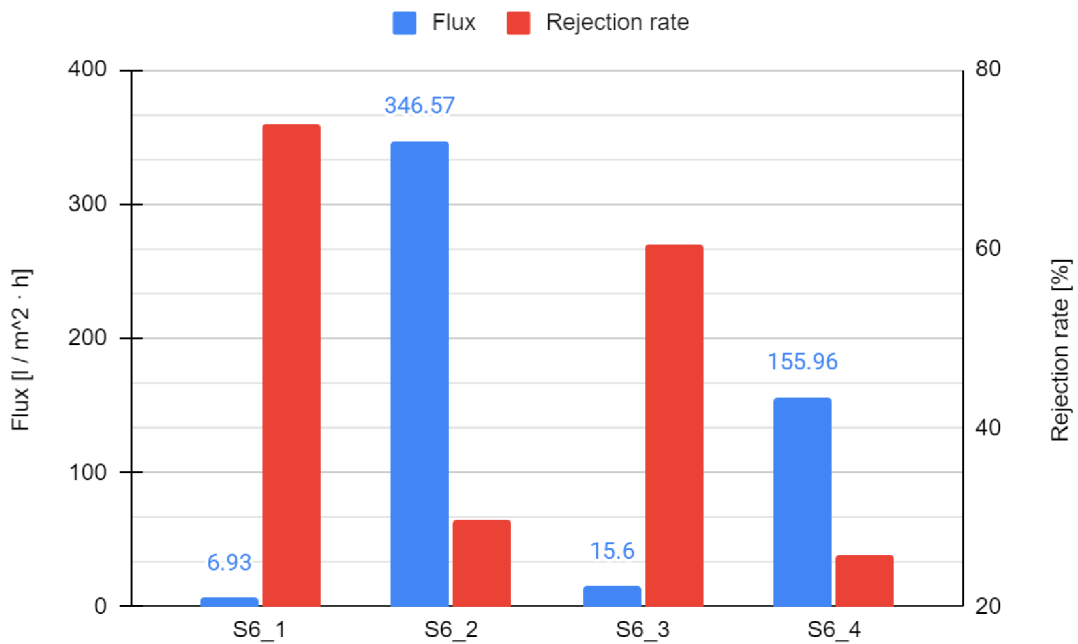


Figure 4.6: Comparison of flux and rejection rates for monomer solution used multiple times in a row

Sample	Solution 1	Solution 2	Contact T S1*	Drying time	Contact T S2*	2nd drying time	Drying conditions	Surfactant conc.	Fresh monomer used
S6_1	2 % EDA	0.2 % TMC	90 s	60 s	90 s	60 s rest	15 min @ 80 °C	0.33 %V Et	Yes
S6_2	2 % EDA	0.2 % TMC	90 s	60 s	90 s	60 s rest	15 min @ 80 °C	0.33 %V Et	No
S6_3	2 % EDA	0.2 % TMC	90 s	60 s	90 s	60 s rest	15 min @ 80 °C	0.035 %w SDS	Yes
S6_4	2 % EDA	0.2 % TMC	90 s	60 s	90 s	60 s rest	15 min @ 80 °C	0.035 %w SDS	No

* Contact times with solutions 1 and 2, respectively.

Table 4.6: Comparison of flux and rejection rates for monomer solution used multiple times in a row

Figure 4.8 compares a commercially available membrane used for desalination and best-performing EDA-based membranes. One commercial material (Whatman® nylon filter) was used as a surrogate for support material, however, a very low rejection rate (7 %), permeability and durability have shown that this material is not suitable for this application and was not tested any further. The commercial membrane shown in Figure 4.8 is a membrane made by Sterlitech. This membrane had a higher rejection rate for the

divalent salt, however, it got out-competed by an EDA-based membrane during the test with a monovalent salt.

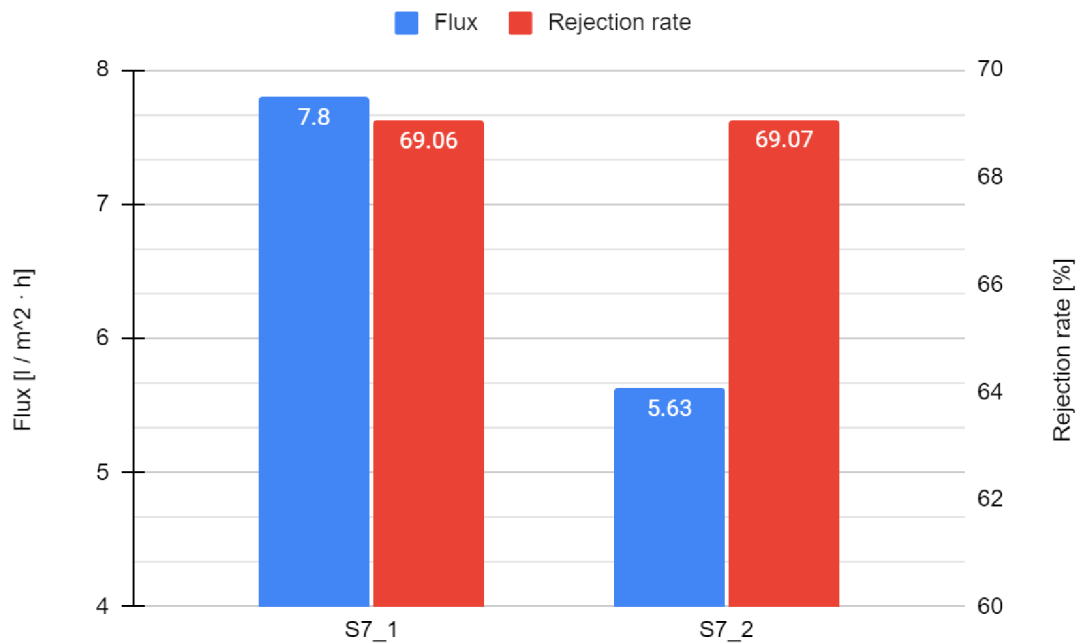


Figure 4.7: Comparison of flux and rejection rates for samples made with a focus on identical conditions

Sample	Solution 1	Solution 2	Contact T S1*	Drying time	Contact T S2*	2nd drying time	Drying cond.	Surfactant conc.	Salt feed
S7_1	2 % EDA	0.2 % TMC	90 s	60 s	90 s	60 s rest	15 min @ 80 °C	0.33 %V Et	MgSO ₄
S7_2	2 % EDA	0.2 % TMC	90 s	60 s	90 s	60 s rest	15 min @ 80 °C	0.33 %V Et	NaCl

* Contact times with solutions 1 and 2, respectively.

Table 4.7: Comparison of flux and rejection rates for samples made with a focus on identical conditions

4.2 Results of pH change

The greatest challenge is accurately determining the rejection rate using the conductivity metre. Adding acid to the feed inevitably increases the conductivity of the solution. While the base conductivity of distilled water is negligible, the base conductivity of the acid-water solution was often higher than the neutral salt feed's. This means more measurement steps were required to obtain the result and thus a more significant error could be introduced.

The electrolytic conductivity of the MgSO₄ solution was measured at 2337 μS/cm before the addition of hydrochloric acid, and it increased to 4000 μS/cm after the acid was added. The conductivity of distilled water with the acid was measured at 1700 μS/cm. After filtering the salt solution through the membrane, the conductivity dropped to 1672 μS/cm.

Based on the decrease in conductivity, it can be estimated that the rejection rate of the salt was 58.2%. However, considering that the conductivity was lowered by 2328 μS/cm compared to the original conductivity of the solution without the acid, the overall rejection rate of the salt could potentially be as high as 99.83%. This suggests that the lower pH had a significant effect on the membrane's rejection capabilities, resulting in a remarkable reduction in the passage of salt ions through the membrane. However, no further tests were able to achieve at least similar values and both the flux and rejection rates were comparable or even worse than in the case of samples tested with neutral feeds. While it has been proven that pH affects EDA-based or EDA-modified membranes no decisive conclusion could have been made [32].

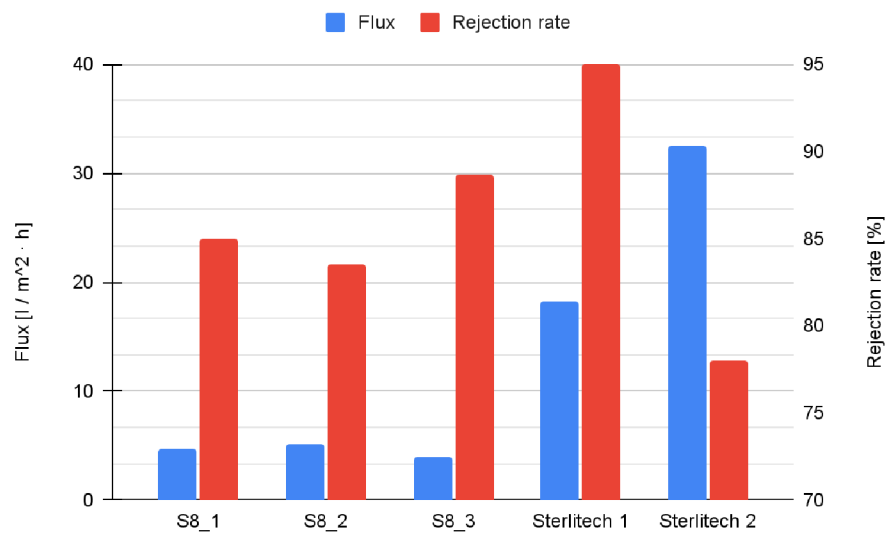


Figure 4.8: Comparison of flux and rejection rates of the best-performing samples with commercially available membranes

Sample	Solution 1	Solution 2	Contact T S1*	Drying time	Contact T S2*	2nd drying time	Drying cond.	Surfactant conc.	Salt feed
S8_1	2 % EDA	0.2 % TMC	90 s	60 s	90 s	60 s rest	15 min @ 80 °C	0.33 %V Et	MgSO ₄
S8_2	2 % EDA	0.2 % TMC	90 s	60 s	90 s	60 s rest	15 min @ 80 °C	0.33 %V Et	NaCl
S8_3	2 % EDA	0.2 % TMC	90 s	60 s	90 s	60 s rest	15 min @ 80 °C	0.33 %V Et	MgSO ₄
Sterlitech 1									MgSO ₄
Sterlitech 2									NaCl

* Contact times with solutions 1 and 2, respectively.

Table 4.8: Comparison of flux and rejection rates of the best-performing samples with commercially available membranes

The next two samples were subjected to a solution with a pH level of 1.7. These samples exhibited very low permeability, around 0.05 ml/min, and demonstrated rejection rates of 67% for NaCl and 77% for MgSO₄.

The second batch of samples was tested at a slightly higher pH of 2.9. In this case, the permeability was notably higher at 10 ml/min, and the rejection rates for both membranes dropped to only 34%. This significantly increased permeability could imply an issue with the membrane itself, potentially stemming from the preparation process. Nevertheless, even the samples with lower permeability showed lower rejection rates compared to other samples tested under neutral pH conditions.

4.3 The Analysis of Film Morphology and Composition using Scanning Electron Microscopy (SEM)

For easier evaluation and higher clarity of the following analysis only seven samples were chosen. These samples include the three best-performing samples and the rest are prepared under different conditions. Chosen samples are listed in Table 4.9.

Sample	Monomer A	Monomer B	Contact A	Rest	Contact B	
A	2 % EDA	0.2 % TMC	90 s	60 s	90 s	
B	2 % EDA	0.2 % TMC	90 s	60 s	90 s	
C	2 % EDA	0.2 % TMC	90 s	60 s	90 s	
D	2.5 % EDA	0.5 % TMC	300 s	60 s	180 s	
E	2 % EDA	0.2 % TMC	90 s	180 s	90 s	
F	2 % EDA	0.2 % TMC	90 s	180 s	90 s	
G	2 % EDA	0.2 % TMC	90 s	180 s	90 s	
Sample	2nd rest	Oven cond.	Flux [LMH]	Rejection	Feed type	Surfactant
A	60 s rest	15 min @ 80 °C	3.89	88.62 %	Mg	0.33 %V Et
B	60 s rest	15 min @ 80 °C	4.77	84.95 %	Mg	0.33 %V Et
C	60 s rest	15 min @ 80 °C	5.19	83.52 %	Na	0.33 %V Et
D	60 s rest	20 min @ 60 °C	8.66	56.8 %	Mg	0.67 %V Et
E		10 min @ 100 °C	Not tested			None
F		10 min @ 100 °C	216	20.2 %	Mg	None
G		10 min @ 100 °C	1080	9.3 %	Mg	None

Table 4.9: List of samples chosen for further analysis

It was challenging to take a cross-section of the samples. Only surface SEM images are taken from selected samples. The SEM images are shown in Table 4.10. The sole distinction between timing A and B lies in the duration of immersion in the first monomer prior to immersion in the second monomer. Timing A is 60 sec while timing B is 180 sec. Apparently, enhancing the waiting time within two monomers influences the structure of the final PA layer. Longer durations mean the first polymer gets dried from the membrane surface which can influence membrane film forming and thickness. Since we were not able to measure the thickness, we can control the differences on the top surface. The first image shows a thicker film layer compared to the last one. The last SEM image shows that the nanofiber support layer is visible.

Moreover, the SEM clearly shows the change in surface morphology by changing the concentration of EDA and TMC monomers. It is expected the higher amount can cause

a thicker PA layer. Based on the experimental results, it can be concluded that the formation of the polyamide selective membrane on the nanofibrous support layer was achieved with success. The leaf-like morphology observed in the polyamide TFC membranes serves as confirmation, as it is a characteristic feature commonly associated with such membranes [37].

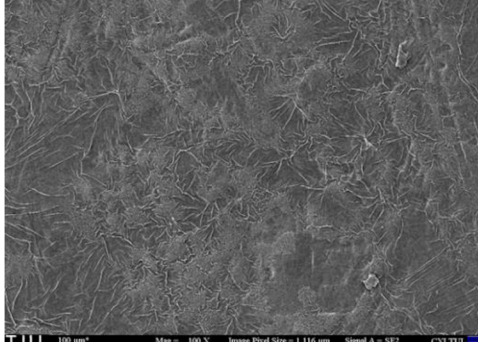
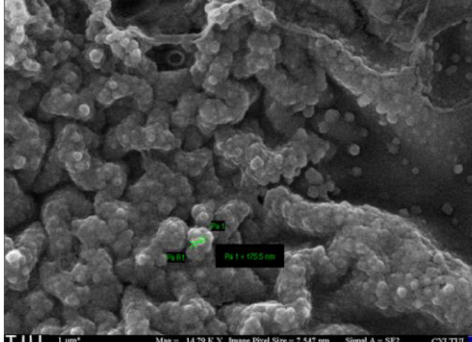
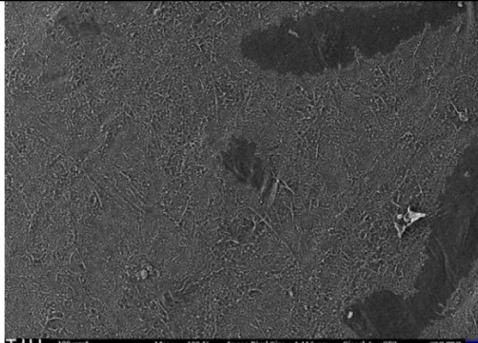
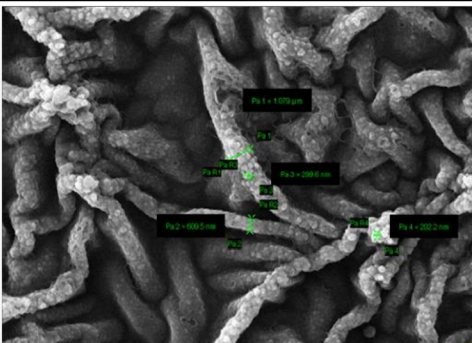
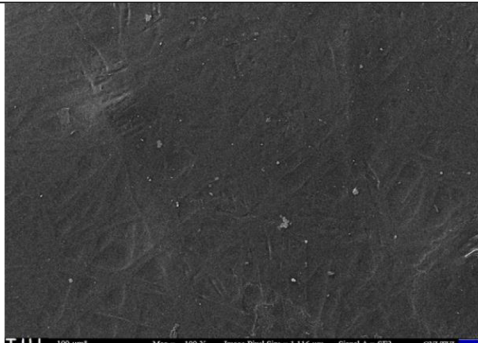
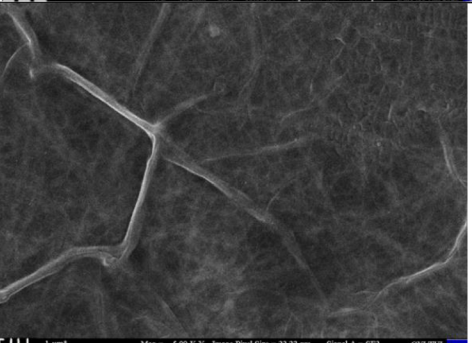
Sample name	SEM	
2%EDA+ 0.2%TMC @ timing A (Sample A)		
2.5%EDA + 0.5%TMC (Sample D)		
2%EDA+ 0.2%TMC @ timing B (Sample E)		

Table 4.10: SEM images of samples A, D and E

4.4 Surface Chemical Property

EDA has an alkane chemical structure with diamine terminal groups. In order to validate the reaction process associated with EDA-TMC, the selective layers of polyamide (PA) are subjected to characterisation using Fourier Transform Infrared Spectroscopy (FTIR), as depicted in Figure 4.9. The presence of a primary amide (amide I, C=O) and

a secondary amide (amide II, N-H) can be identified by the characteristic peaks observed at 1636 and 1534 cm^{-1} , respectively. In addition to the aforementioned typical bands, it is crucial to note that the bands observed at around 3300 cm^{-1} can be attributed to the vibrations associated with N-H stretching. Figure 4.9 demonstrates the successful creation of a selective layer for polyamide (PA). The findings align with the existing literature [38–40].

The residual hexane has been observed on the sample. Prominent absorption bands corresponding to the stretching vibrations of C-H bonds are observed within the wavenumber range of 2880 to 2960 cm^{-1} , while the deformation vibrations of C-H bonds in the CH₂ and CH₃ groups within hexane are evident at a wavenumber of 1432 cm^{-1} .

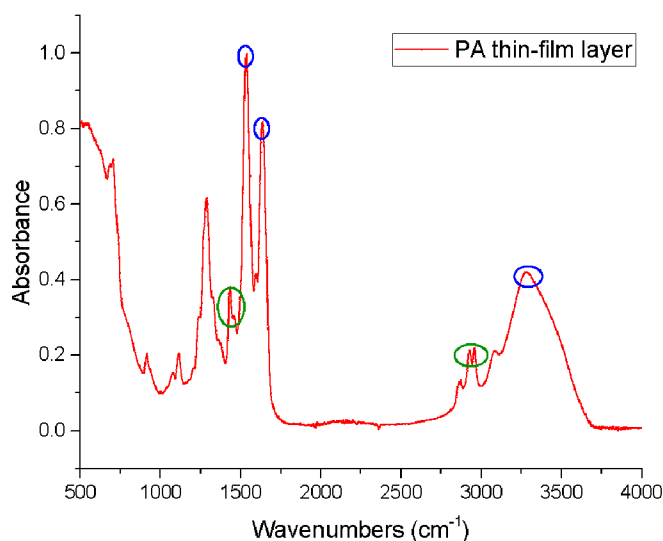
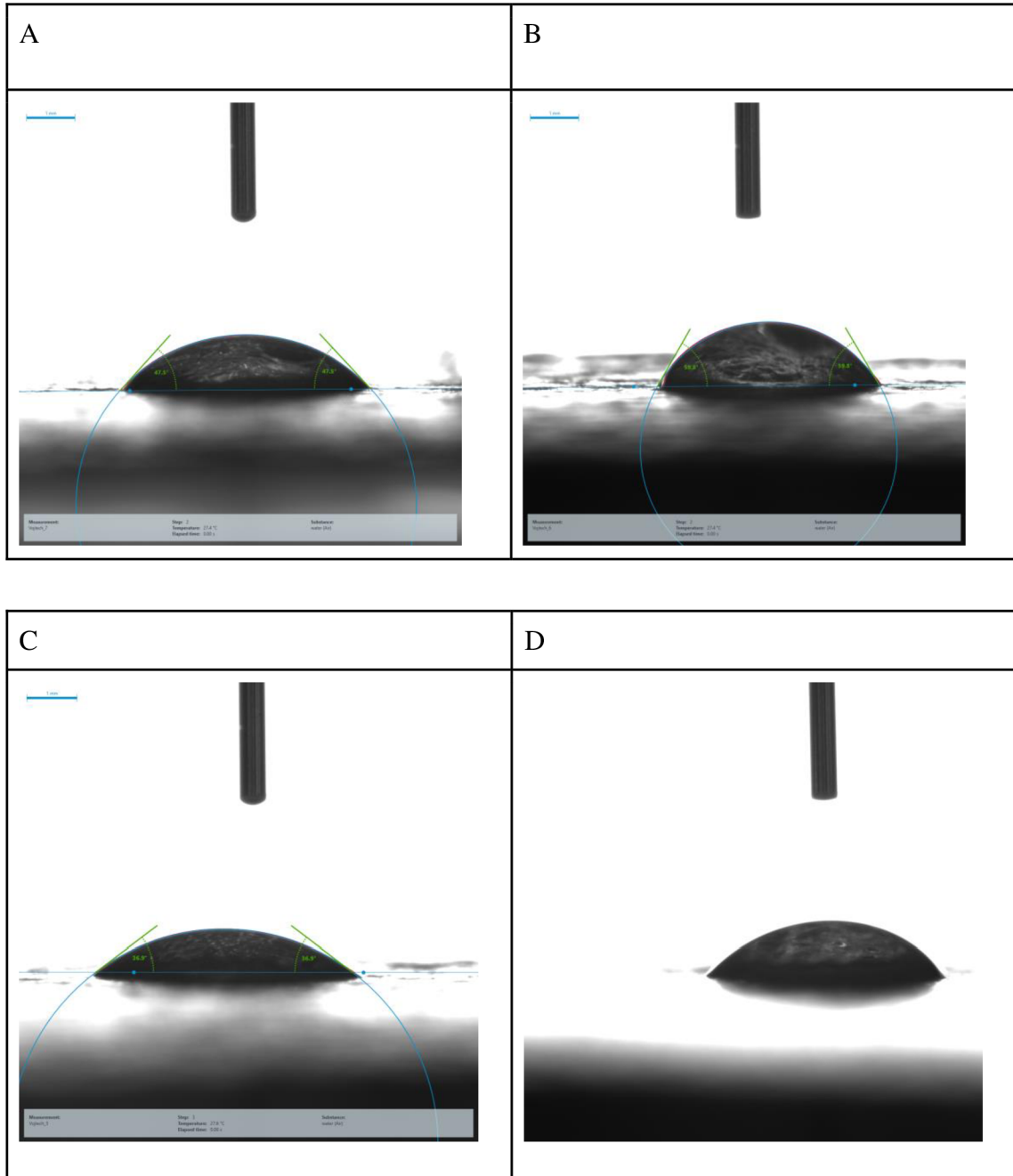


Figure 4.9: FTIR images EDA/TMC formed PA thin-film

4.5 Contact angle

The contact angle of the membrane can be affected by various parameters, including the concentration of monomers, duration of the reaction, type of organic solution used, and posttreatment conditions, among others, throughout the interfacial polymerisation (IP) reaction process. The contact angle measurements are depicted in Table 4.11 and precise values are listed in Table 4.12. All samples showed hydrophilic properties with WCA less than 90°. A noticeable decrease in contact angle was achieved compared to the base support material. The contact angle of the support material without the PA layer was

approximately 118° . Nevertheless, the contact angle value reported in this study is within the range of contact angles previously recorded for the TFC membrane [37].



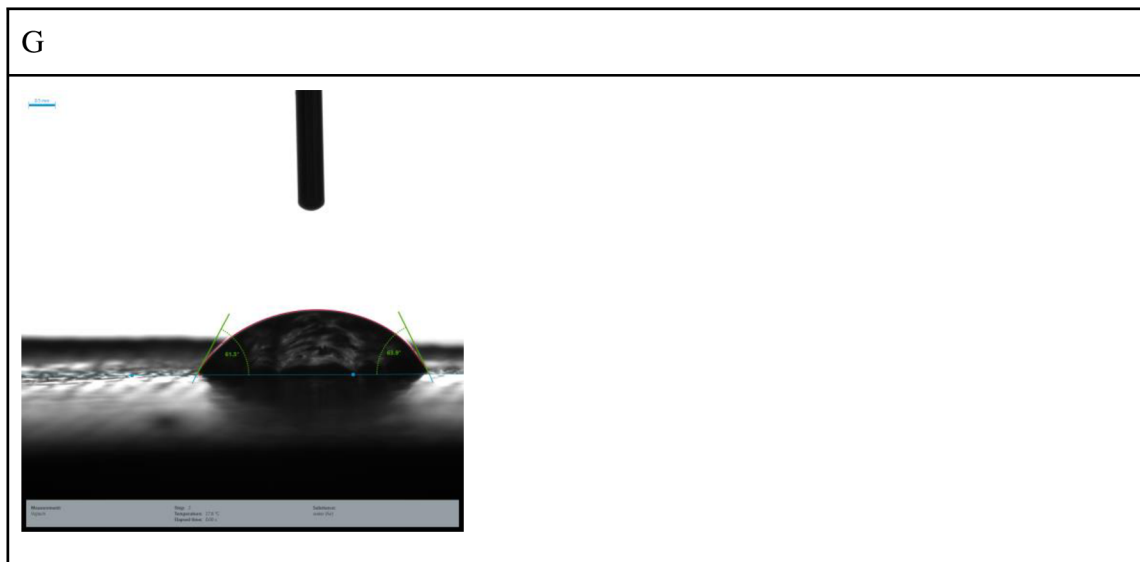
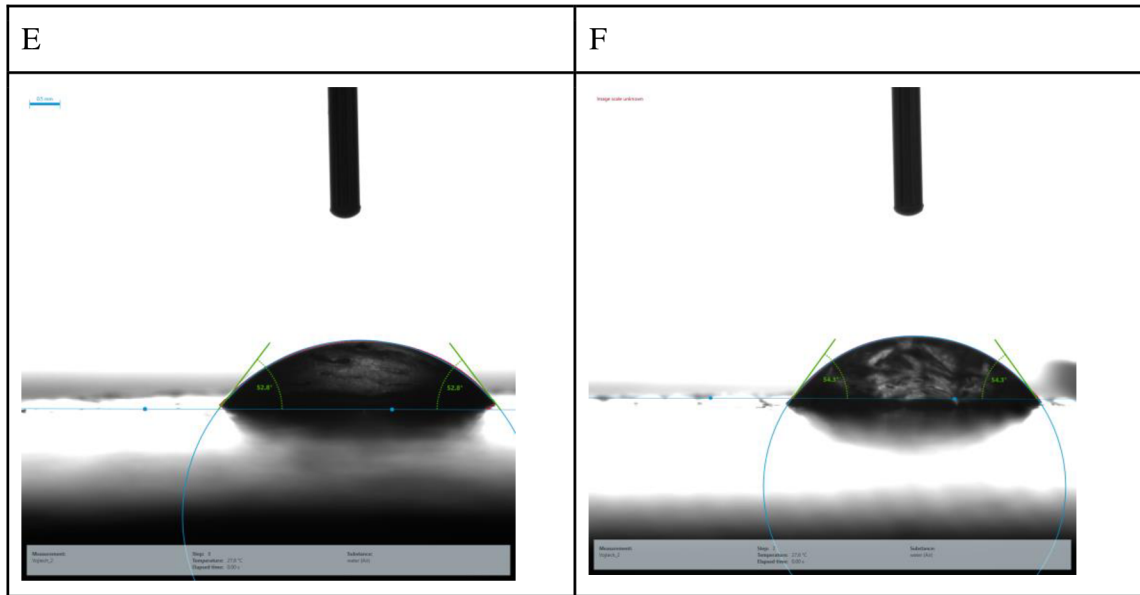


Table 4.11: Images of contact angles of chosen samples

Sample	Temperature [°C]	Mean CA [°]
Sample A	27.4	48.83 ± 2.27
Sample B	27.4	55.64 ± 2.84
Sample C	27.6	38.57 ± 4.28
Sample D	27.7	56.44 ± 3.97
Sample E	27.8	46.44 ± 1.32
Sample F	27.7	52.29 ± 3.05
Sample G	27.6	49.82 ± 5.35

Table 4.12: List of contact angle values of chosen samples

4.6 Further research

More testing of the influence of pH on EDA-based membranes is undoubtedly needed. Determining a point of the best compromise between permeability and rejection should be the focus. Another focus should be on the modifications of the support materials and the compatibility of various support materials with different monomers as well as the suitability of said support materials for different applications.

Further research will be focused on the modification of the EDA-based membranes with other monomers or nanoparticles. The reason is the need for higher membrane selectivity and higher permeability.

5. Conclusion

In conclusion, this thesis conducted an extensive investigation into the fabrication and improvement of TFC membranes intended for the efficient separation of saline aqueous solutions. The major goal has been achieved by implementing a systematic series of procedure adjustments to improve rejection rates while maintaining satisfactory permeability properties. The rejection efficiencies of both NaCl and MgSO₄ did not meet the expected standards during the earliest phase of research. Following this, a methodical series of modifications was commenced, including adjustments in the concentration of monomers, durations of reactions, and the interactions between different monomers. Despite the difficulties and variations observed, the previously mentioned interventions have brought to light the adaptability of membrane efficacy. This observation indicates that adjustable parameters can be effective in overcoming the inherent limitations in the performance of polymer substrates.

Adjustments were made to the preparation process of the support material in the succeeding phases of optimisation, with the primary objective of improving the membrane's uniformity and minimising any surface defects. The application of pretreatment techniques involving ethanol and SDS has yielded promising results, resulting in observable increases in rejection efficiency. The third phase of optimisation centred on the adjusting of solution concentrations, drying kinetics, and preparation

methods. In particular, a pattern emerged in which the second sample in each pair consistently had significantly lower rejection metrics, necessitating a revision of the preparation process.

After judicious adjustments, the final set of samples exhibited remarkable NaCl and MgSO₄ rejection efficiencies. Under optimal configurations, these results indicated that rejection efficiencies as high as 84.95 and 83.53 percent are attainable. In addition, the effects of pH reduction on membrane performance were investigated. Remarkably, decreased pH values led to a remarkable improvement in rejection capabilities, most likely as a result of a decrease in salt ion permeability through the membrane matrix.

This thesis has successfully accomplished its primary objective of fabricating TFC membranes that demonstrate proficiency in the separation of saline aqueous compositions. Through rigorous refinements and methodological modifications, the investigation has not only revealed the complex interaction of various parameters on membrane performance but also demonstrated the possibility of attaining higher rejection efficiencies in tandem with higher permeability indices. The knowledge gained in this study will unquestionably broaden the scope of membrane technology, thereby increasing the likelihood of its application in desalination and similar separation projects.

References

- [1] *Consequences of climate change*. Website. Available from: https://climate.ec.europa.eu/climate-change/consequences-climate-change_en. [viewed 2023-08-18].
- [2] Water as a Solvent: Properties & Importance | StudySmarter. online. In: *StudySmarter UK*. Available from: <https://www.studysmarter.co.uk/explanations/biology/chemistry-of-life/water-as-a-solvent/>. [viewed 2023-08-18].
- [3] SANTI, Claudio; Raquel G. JACOB; Bonifacio MONTI; Luana BAGNOLI; Luca SANCINETO et al. Water and Aqueous Mixtures as Convenient Alternative Media for Organoselenium Chemistry. online. *Molecules*, vol. 21 (2016), no. 11, p. 1482. Available from: <https://doi.org/10.3390/molecules21111482>.
- [4] *Photosynthesis*. Website. Available from: <https://education.nationalgeographic.org/resource/photosynthesis>. [viewed 2023-08-18].
- [5] *Reducing the Greenhouse Gas Emissions of Water and Sanitation Services: Overview of emissions and their potential reduction illustrated by utility know-how*. online. IWA Publishing, 2022. Available from: <https://doi.org/10.2166/9781789063172>.
- [6] FRITZMANN, C.; J. LÖWENBERG; T. WINTGENS and T. MELIN. State-of-the-art of reverse osmosis desalination. online. *Desalination*, vol. 216 (2007), no. 1, pp. 1–76. Available from: <https://doi.org/10.1016/j.desal.2006.12.009>.
- [7] WARSINGER, David M.; Karan H. MISTRY; Kishor G. NAYAR; Hyung Won CHUNG and John H. LIENHARD. Entropy Generation of Desalination Powered by Variable Temperature Waste Heat. online. *Entropy*, vol. 17 (2015), no. 11, pp. 7530–7566. Available from: <https://doi.org/10.3390/e17117530>.
- [8] NATH, KAUSHIK. *MEMBRANE SEPARATION PROCESSES*. PHI Learning Pvt. Ltd., 2017. ISBN 978-81-203-5291-9. Google-Books-ID: 1VrWDQAAQBAJ.
- [9] YALCINKAYA, Baturalp. *Nanofiltration membranes based on nanofibrous material*. Dissertation. Liberec: Technická univerzita v Liberci, Fakulta textilní, 2016.
- [10] VAN DER BRUGGEN, Bart; Carlo VANDECASTEELE; Tim VAN GESTEL; Wim DOYEN and Roger LEYSEN. A review of pressure-driven membrane processes in wastewater treatment and drinking water production. online. *Environmental Progress*, vol. 22 (2003), no. 1, pp. 46–56. Available from: <https://doi.org/10.1002/ep.670220116>.
- [11] YUAN, Hongmei; Jianguo LIU; Xinghua ZHANG; Lungang CHEN; Qi ZHANG et al. Recent advances in membrane-based materials for desalination and gas separation. online. *Journal of Cleaner Production*, vol. 387 (2023), p. 135845. Available from: <https://doi.org/10.1016/j.jclepro.2023.135845>.
- [12] ZENG, Haoze; Shanshan HE; Seyed Saeid HOSSEINI; Bin ZHU and Lu SHAO. Emerging nanomaterial incorporated membranes for gas separation and pervaporation towards energetic-efficient applications. online. *Advanced Membranes*, vol. 2 (2022), p. 100015. Available from: <https://doi.org/10.1016/j.advmem.2021.100015>.
- [13] TAO, Quanzheng; Martin DAHLQVIST; Jun LU; Sankalp KOTA; Rahele MESHKIAN et al. Two-dimensional Mo_{1.33}C MXene with divacancy ordering prepared from parent 3D laminate with in-plane chemical ordering. online. *Nature Communications*, vol. 8 (2017), no. 1, p. 14949. Available from: <https://doi.org/10.1038/ncomms14949>.
- [14] NAGUIB, Michael; Vadym N. MOCHALIN; Michel W. BARSOUM and Yury GOGOTSI. 25th Anniversary Article: MXenes: A New Family of Two-Dimensional Materials. online. *Advanced Materials*, vol. 26 (2014), no. 7, pp. 992–1005. Available from: <https://doi.org/10.1002/adma.201304138>.
- [15] PERREAULT, François; Andreia FONSECA DE FARIA and Menachem ELIMELECH. Environmental applications of graphene-based nanomaterials. online. *Chemical Society Reviews*, vol. 44 (2015), no. 16, pp. 5861–5896. Available from: <https://doi.org/10.1039/C5CS00021A>.
- [16] NAIR, R. R.; H. A. WU; P. N. JAYARAM; I. V. GRIGORIEVA and A. K. GEIM.

- Unimpeded Permeation of Water Through Helium-Leak-Tight Graphene-Based Membranes. online. *Science*, vol. 335 (2012), no. 6067, pp. 442–444. Available from: <https://doi.org/10.1126/science.1211694>.
- [17] LI, Meng-Na; Xiu-Juan CHEN; Zhang-Hong WAN; Shu-Guang WANG and Xue-Fei SUN. Forward osmosis membranes for high-efficiency desalination with Nano-MoS₂ composite substrates. online. *Chemosphere*, vol. 278 (2021), p. 130341. Available from: <https://doi.org/10.1016/j.chemosphere.2021.130341>.
- [18] LU, Xinglin; Uri R. GABINET; Cody L. RITT; Xunda FENG; Akshay DESHMUKH et al. Relating Selectivity and Separation Performance of Lamellar Two-Dimensional Molybdenum Disulfide (MoS₂) Membranes to Nanosheet Stacking Behavior. online. *Environmental Science & Technology*, vol. 54 (2020), no. 15, pp. 9640–9651. Available from: <https://doi.org/10.1021/acs.est.0c02364>.
- [19] LI, Xuesong; Qing LI; Wangxi FANG; Rong WANG and William B. KRANTZ. Effects of the support on the characteristics and permselectivity of thin film composite membranes. online. *Journal of Membrane Science*, vol. 580 (2019), pp. 12–23. Available from: <https://doi.org/10.1016/j.memsci.2019.03.003>.
- [20] PETERSEN, Robert J. Composite reverse osmosis and nanofiltration membranes. online. *Journal of Membrane Science*, vol. 83 (1993), no. 1, pp. 81–150. Available from: [https://doi.org/10.1016/0376-7388\(93\)80014-O](https://doi.org/10.1016/0376-7388(93)80014-O).
- [21] SINGH, Puyam S.; S.V. JOSHI; J.J. TRIVEDI; C.V. DEVMURARI; A. Prakash RAO et al. Probing the structural variations of thin film composite RO membranes obtained by coating polyamide over polysulfone membranes of different pore dimensions. online. *Journal of Membrane Science*, vol. 278 (2006), no. 1–2, pp. 19–25. Available from: <https://doi.org/10.1016/j.memsci.2005.10.039>.
- [22] GHOSH, Asim K. and Eric M.V. HOEK. Impacts of support membrane structure and chemistry on polyamide–polysulfone interfacial composite membranes. online. *Journal of Membrane Science*, vol. 336 (2009), no. 1–2, pp. 140–148. Available from: <https://doi.org/10.1016/j.memsci.2009.03.024>.
- [23] LI, Xuesong; Chun Heng LOH; Rong WANG; Wentalia WIDJAJANTI and Jaume TORRES. Fabrication of a robust high-performance FO membrane by optimizing substrate structure and incorporating aquaporin into selective layer. online. *Journal of Membrane Science*, vol. 525 (2017), pp. 257–268. Available from: <https://doi.org/10.1016/j.memsci.2016.10.051>.
- [24] LIN, Lin; Rene LOPEZ; Guy Z. RAMON and Orlando CORONELL. Investigating the void structure of the polyamide active layers of thin-film composite membranes. online. *Journal of Membrane Science*, vol. 497 (2016), pp. 365–376. Available from: <https://doi.org/10.1016/j.memsci.2015.09.020>.
- [25] ZHOU, Fanglei; Huynh Ngoc TIEN; Qiaobei DONG; Weiwei L. XU; Huazheng LI et al. Ultrathin, ethylenediamine-functionalized graphene oxide membranes on hollow fibers for CO₂ capture. online. *Journal of Membrane Science*, vol. 573 (2019), pp. 184–191. Available from: <https://doi.org/10.1016/j.memsci.2018.11.080>.
- [26] AHMADIJOKANI, Farhad; Shima TAJAHMADI; Addie BAHI; Hossein MOLAVI; Mashallah REZAKAZEMI et al. Ethylenediamine-functionalized Zr-based MOF for efficient removal of heavy metal ions from water. online. *Chemosphere*, vol. 264 (2021), p. 128466. Available from: <https://doi.org/10.1016/j.chemosphere.2020.128466>.
- [27] JANG, Jaewon; Yesol KANG; Kyunghoon JANG; Suhun KIM; Sang-Soo CHEE et al. Ti₃C₂TX-Ethylenediamine nanofiltration membrane for high rejection of heavy metals. online. *Chemical Engineering Journal*, vol. 437 (2022), p. 135297. Available from: <https://doi.org/10.1016/j.cej.2022.135297>.
- [28] LI, Qiang; Xiaotai ZHANG; Hui YU; Huifeng ZHANG and Jihua WANG. A facile surface modification strategy for improving the separation, antifouling and antimicrobial performances of the reverse osmosis membrane by hydrophilic and Schiff-base functionalizations. online. *Colloids and Surfaces A: Physicochemical and Engineering Aspects*, vol. 587 (2020), p. 124326. Available from: <https://doi.org/10.1016/j.colsurfa.2019.124326>.

- [29] AMASHAEV, R. R.; I. M. ABDULAGATOV; M. Kh. RABADANOV and A. I. ABDULAGATOV. Molecular Layer Deposition and Pyrolysis of Polyamide Films on Si(111) with Formation of β -SiC. online. *Russian Journal of Physical Chemistry A*, vol. 95 (2021), no. 7, pp. 1439–1448. Available from: <https://doi.org/10.1134/S0036024421070049>.
- [30] SEAH, Mei Qun; Woei Jye LAU; Pei Sean GOH; Hui-Hsin TSENG; Roswanira Abdul WAHAB et al. Progress of Interfacial Polymerization Techniques for Polyamide Thin Film (Nano)Composite Membrane Fabrication: A Comprehensive Review. online. *Polymers*, vol. 12 (2020), no. 12, p. 2817. Available from: <https://doi.org/10.3390/polym12122817>.
- [31] PHAM, Minh-Xuan; Thu MINH LE; Thien TRONG TRAN; Huynh Ky Phuong HA; Mai THANH PHONG et al. Fabrication and characterization of polyamide thin-film composite membrane via interfacial polycondensation for pervaporation separation of salt and arsenic from water. online. *RSC Advances*, vol. 11 (2021), no. 63, pp. 39657–39665. Available from: <https://doi.org/10.1039/D1RA07492J>.
- [32] ANG, Micah Belle Marie Yap; Yi-Ling WU; Min-Yi CHU; Ping-Han WU; Yu-Hsuan CHIAO et al. Nanofiltration Membranes Formed through Interfacial Polymerization Involving Cycloalkane Amine Monomer and Trimesoyl Chloride Showing Some Tolerance to Chlorine during Dye Desalination. online. *Membranes*, vol. 12 (2022), no. 3, p. 333. Available from: <https://doi.org/10.3390/membranes12030333>.
- [33] LAU, W. J.; A. F. ISMAIL; N. MISDAN and M. A. KASSIM. A recent progress in thin film composite membrane: A review. online. *Desalination*, vol. 287 (2012), pp. 190–199. Available from: <https://doi.org/10.1016/j.desal.2011.04.004>.
- [34] IDARRAGA-MORA, Jaime; Anthony CHILDRESS; Parker FRIEDEL; David LADNER; Apparao RAO et al. Role of Nanocomposite Support Stiffness on TFC Membrane Water Permeance. online. *Membranes*, vol. 8 (2018), p. 111. Available from: <https://doi.org/10.3390/membranes8040111>.
- [35] SAHA, N. K. and S. V. JOSHI. Performance evaluation of thin film composite polyamide nanofiltration membrane with variation in monomer type. online. *Journal of Membrane Science*, vol. 342 (2009), no. 1, pp. 60–69. Available from: <https://doi.org/10.1016/j.memsci.2009.06.025>.
- [36] ROSLAN, Jumardi; Siti Mazlina MUSTAPA KAMAL; Khairul Faezah MD. YUNOS and Norhafizah ABDULLAH. Evaluation on performance of dead-end ultrafiltration membrane in fractionating tilapia by-product protein hydrolysate. online. *Separation and Purification Technology*, vol. 195 (2018), pp. 21–29. Available from: <https://doi.org/10.1016/j.seppur.2017.11.020>.
- [37] KADHOM, Mohammed; Jun YIN and Baolin DENG. A Thin Film Nanocomposite Membrane with MCM-41 Silica Nanoparticles for Brackish Water Purification. online. *Membranes*, vol. 6 (2016), no. 4, p. 50. Available from: <https://doi.org/10.3390/membranes6040050>.
- [38] XIONG, Shu; Jian ZUO; Yuan Gui MA; Lifan LIU; Hao WU et al. Novel thin film composite forward osmosis membrane of enhanced water flux and anti-fouling property with N-[3-(trimethoxysilyl) propyl] ethylenediamine incorporated. online. *Journal of Membrane Science*, vol. 520 (2016), pp. 400–414. Available from: <https://doi.org/10.1016/j.memsci.2016.07.034>.
- [39] YU, Chung-Hao; Irdham KUSUMAWARDHANA; Juin-Yih LAI and Ying-Ling LIU. PTFE/polyamide thin-film composite membranes using PTFE films modified with ethylene diamine polymer and interfacial polymerization: Preparation and pervaporation application. online. *Journal of Colloid and Interface Science*, vol. 336 (2009), no. 1, pp. 260–267. Available from: <https://doi.org/10.1016/j.jcis.2009.03.052>.
- [40] ZHOU, Chenxu; Shunxin QI; Ping ZHU; Ying ZHAO; Yizhuang XU et al. The methylene infrared vibration and dielectric behavior monitored by amide group arrangement for long chain polyamides. online. *Polymer*, vol. 190 (2020), p. 122231. Available from: <https://doi.org/10.1016/j.polymer.2020.122231>.